

1 **Intercomparison of detection and quantification methods for methane emissions from**  
2 **the natural gas distribution network in Hamburg, Germany**

3  
4 Hossein Maazallahi<sup>1, 2</sup>, Antonio Delre<sup>3</sup>, Charlotte Scheutz<sup>3</sup>, Anders M. Fredenslund<sup>3</sup>, Stefan  
5 Schwietzke<sup>4</sup>, Hugo Denier van der Gon<sup>2</sup>, Thomas Röckmann<sup>1</sup>

6  
7 <sup>1</sup>*Institute for Marine and Atmospheric research Utrecht (IMAU), Utrecht University (UU),*  
8 *Utrecht, The Netherlands*

9 <sup>2</sup>*Netherlands Organisation for Applied Scientific Research (TNO), Utrecht, the Netherlands*

10 <sup>3</sup>*Department of Environmental Engineering, Technical University of Denmark (DTU),*  
11 *Lyngby, Denmark*

12 <sup>4</sup>*Environmental Defense Fund (EDF), Berlin, Germany*

13  
14 **Correspondence:** Hossein Maazallahi (h.maazallahi@uu.nl)

15  
16 **Abstract:**

17 In August and September 2020, three different measurement methods for quantifying methane  
18 (CH<sub>4</sub>) emissions from leaks in urban gas distribution networks were applied and compared in  
19 Hamburg, Germany: the “mobile”, “tracer release” and “suction” methods.  
20 The mobile and tracer release methods determine emission rates to the atmosphere from  
21 measurements of CH<sub>4</sub> mole fractions in the ambient air, and the tracer release method also  
22 includes measurement of a gaseous tracer. The suction method determines emission rates by  
23 pumping air out of the ground using soil probes that are placed above the suspected leak  
24 location. The quantitative intercomparison of the emission rates from the three methods at a  
25 small number of locations is challenging because of limitations of the different methods at  
26 different types of leak locations.

27 The mobile method was designed to rapidly quantify the average or total emission rate of many  
28 gas leaks in a city, but it yields a large emission rate uncertainty for individual leak locations.  
29 Emission rates determined for individual leak locations with the tracer release technique are  
30 more precise because the simultaneous measurement of the tracer released at a known rate at  
31 the emission source eliminates many of the uncertainties encountered with the mobile method.  
32 Nevertheless, care must be taken to properly collocate the tracer release and the leak emission  
33 points to avoid biases in emission rate estimates. The suction method could not be completed  
34 or applied at locations with widespread subsurface CH<sub>4</sub> accumulation, or due to safety  
35 measures. While the number of gas leak locations in this study is small, we observe a  
36 correlation between leak emission rate and subsurface accumulation. Wide accumulation  
37 places leaks into a safety category that requires immediate repair so that the suction method  
38 cannot be applied to these larger leaks in routine operation. This introduced a sampling bias  
39 for the suction method in this study towards the low-emission leaks, which do not require  
40 immediate repair action. Given that this study is based on random sampling, such a sampling  
41 bias may also exist for the suction method outside of this study. While an investigation of the  
42 causal relationship between safety category and leak size is beyond the scope of this study, on  
43 average higher emission rates were observed from all the three measurement-based  
44 quantification methods for leaks with higher safety priority compared to the leaks with lower  
45 safety concern. The leak locations where the suction method could not be applied were the  
46 biggest emitters as confirmed by the emission rate quantifications using mobile and tracer  
47 methods and an engineering method based on leak’s diameter, pipeline overpressure and depth  
48 at which the pipeline is buried. The corresponding sampling bias for the suction technique led  
49 to a low bias in derived emission rates in this study. It is important that future studies using the

50 suction method account for any leaks not quantifiable with this method in order to avoid biases,  
51 especially when used to inform emission inventories.  
52

# 53 1 Introduction

54  
55 Natural gas combustion has a lower carbon footprint than combustion of other fossil fuel  
56 sources for the same thermal output (EIA, 2021). However, fugitive methane (CH<sub>4</sub>) emissions  
57 can significantly turn the balance in terms of climate impact (Alvarez et al., 2012) because the  
58 global warming potential of CH<sub>4</sub> over a 20-year time scale is 84 times higher than that of carbon  
59 dioxide (CO<sub>2</sub>) (Myhre et al., 2013). The atmospheric abundance of CH<sub>4</sub> has increased about  
60 2.5-fold since the pre-industrial era (Bousquet et al., 2006). Following a short period of stable  
61 levels after the year 2000, atmospheric CH<sub>4</sub> has continued to increase since 2006. Worden et  
62 al (2017) concluded that about 50 to 80% of the post-2006 increase originated from fossil  
63 sources and Jackson et al. (2020) attributed the accelerated increase of 6 – 13 ppb yr<sup>-1</sup> from  
64 2014 to 2017 (Nisbet et al., 2019), equally to the emission increase from fossil and agriculture  
65 sectors.  
66

67 Gas distribution networks in cities are subject to maintenance programs by the operators to  
68 detect and fix leakages that occur, as CH<sub>4</sub> is an incendiary gas and can be explosive at mixing  
69 ratios between 4 and 16% in ambient air (DVGW, 2022). Since the safe operation of the  
70 distribution network and leak repair is the primary objective of this maintenance, quantification  
71 of emissions from leakages is rarely performed. The absence of regulations on CH<sub>4</sub> emissions  
72 is another reason why leak rates are not routinely quantified, however CH<sub>4</sub> emissions from the  
73 energy sector need to be addressed properly within the EU CH<sub>4</sub> strategy by 2050 (EC, 2020).  
74 Nevertheless, from the perspective of climate change and possible mitigation options, it is  
75 important that emissions from gas leakages are (i) quickly detected and fixed and (ii) well  
76 quantified. Weller et al. (2020) and Alvarez et al. (2018) respectively reported 5 and 1.6 times  
77 higher CH<sub>4</sub> emissions from leaks in the US gas distribution network based on such observations  
78 compared to the national inventory reports.  
79

80 Leaks from buried pipelines can be due to corrosion or failure/defects in joints or materials  
81 (EPA, 1996). When a leak occurs on a buried urban gas pipeline, the gas will generally  
82 accumulate in the air space below the surface and then find its path to the atmosphere through  
83 a single or several surface outlets. The outlets can be either unpaved soil surfaces, cracks in the  
84 road or pavements, or associated with different types of cavities (manholes, communication  
85 covers, rain drains, etc.). The major outlet is generally the one with the highest overall  
86 permeability for gas released from the buried natural gas pipeline. On the way from the leak  
87 location on a buried pipeline to the atmosphere through outlets, CH<sub>4</sub> may be oxidized by  
88 methanotrophs in the soil and/or merge with CH<sub>4</sub> from other sources, e.g. biogenic CH<sub>4</sub>  
89 emissions from sewage systems.  
90

91 Routine leak surveys in Germany are conducted by walking with handheld CH<sub>4</sub> sensors above  
92 buried pipelines, referred to as the carpet method (DVGW, 2019). The success of leak detection  
93 with the carpet method depends primarily on soil permeability (Ulrich et al., 2019), which is  
94 influenced by soil moisture, texture, soil organic content and the location of the groundwater  
95 table (Wiesner et al., 2016). Based on risk of explosion, gas leaks are classified into four types:  
96 A1, A2, B and C (DVGW, 2019). This classification is based on the accumulation of CH<sub>4</sub> in  
97 cavities (e.g. manholes, rain drains, etc.) or buildings and the distance of gas leaks to buildings  
98 and cavities. If natural gas leaks into buildings or cavities, the leak classifies as A1, and it must

99 be repaired immediately to minimize explosion risk. If the gas leak has a distance up to 1 m to  
100 buildings and does not fill cavities, it is classified as A2, and it must be fixed within a week. If  
101 the distance is between 1 to 4 m to buildings, the leak is classified as B and the repair time  
102 window is three months, and if the distance is more than 4 m then, the leak is considered as C  
103 category and can be fixed according to the scheduled repair plan. There are 6,500 km of low  
104 pressure and 250 km of medium pressure gas pipelines in Hamburg which are monitored every  
105 4 years with the carpet method based on the national regulations in Germany. Gas leaks in  
106 cities are not quantified and thus also not a parameter affecting the course of action. Moreover,  
107 high pressure pipelines are monitored on an annual basis with additional helicopter-based  
108 measurement platforms.

109  
110 In recent years, mobile measurement methods using vehicles with fast and high-precision laser  
111 instrumentation have been established for leak detection and emission quantification in  
112 numerous cities (Jackson et al., 2014; von Fischer et al., 2017; Weller et al., 2018; Keyes et al.,  
113 2020; Ars et al., 2020; Maazallahi et al., 2020; Defratyka et al., 2021; Luetschwager et al.,  
114 2021; Fernandez et al., 2022). In-situ measurements of atmospheric CH<sub>4</sub> from mobile vehicles  
115 are used to pinpoint and quantify CH<sub>4</sub> emission sources at street level in urban areas. The  
116 mobile method was calibrated using above-ground controlled release experiments, in which  
117 known amounts of CH<sub>4</sub> were released from gas cylinders (Weller et al., 2019). Simultaneous  
118 measurements of carbon dioxide (CO<sub>2</sub>) and ethane (C<sub>2</sub>H<sub>6</sub>) can provide valuable additional  
119 information for attributing CH<sub>4</sub> sources (Maazallahi et al., 2020). A characteristic of the  
120 resulting emissions distribution from gas distribution grids in cities is the existence of a few  
121 leak locations with very high leak rates, up to 100 L min<sup>-1</sup>, resulting in a right-skewed leak  
122 emission rate distribution (Weller et al., 2020). Usually about 10% of the leaks are responsible  
123 for between 30% to 70% of the emissions (Weller et al., 2019; Maazallahi et al., 2020).  
124 Therefore, the CH<sub>4</sub> emission from the gas distribution system can be reduced very effectively  
125 if the largest leaks can be found and fixed quickly, thus augmenting the routine leak detection  
126 (carpet method) and repair programs with the mobile method.

127  
128 The tracer dispersion method is another method to quantify CH<sub>4</sub> emissions from point and area  
129 sources. In this method, a tracer gas is released at a known rate close to the outlet of the gas  
130 leak, and both tracer and target gas mixing ratios are measured downwind. From these  
131 measurements and the known tracer gas release rate, the target gas emission rate can be  
132 determined with an uncertainty of ± 15% (Lamb et al., 1995) or less than 20% (Fredenslund et  
133 al., 2019). Lamb et al. (2015) applied the tracer method to quantify leaks from urban  
134 underground pipelines where they reported moderate agreement (± 50%) to excellent  
135 agreement (± 5%) between the tracer and high-flow sampler method. In the high-flow sampler  
136 method, air was drawn at a flow rate of about 0.2 m<sup>3</sup> min<sup>-1</sup> through a flexible enclosure which  
137 covered a leak from a component completely. In this method, CH<sub>4</sub> mixing ratio was measured  
138 with catalytic oxidation and thermal conductivity hydrocarbon sensors and a thermal flow  
139 meter was used to determine gas flow.

140  
141 Another approach to quantify underground leak rates from buried gas pipelines is the so-called  
142 suction method. In this method air is pumped out of the ground at a known rate via probes  
143 surrounding the underground leaks until an equilibrium CH<sub>4</sub> mixing ratio is reached in air out-  
144 flow, from which the CH<sub>4</sub> leak rate can be calculated. In Germany, this approach is applied to  
145 a limited number of leak locations, which do not have to be repaired immediately or within 1  
146 week. Suction measurements normally find leak rates that are < 2 L min<sup>-1</sup> (E.ON, personal  
147 communication, 2020). The reported uncertainty range of this method is ± 10% based on 23  
148 measurements in the 1990s (E.ON, personal communication, 2020). The discrepancy between

149 these rather low leak rates compared to leak rates inferred with the mobile method calls for  
150 further investigation, since the suction method is also employed to derive network-wide  
151 emission factors for the German country-wide gas distribution network (Federal Environment  
152 Agency, 2020).

153  
154 Hendrick et al. (2016) used surface flux chamber measurements carried out between 2012 and  
155 2014 to estimate gas leak rates from 100 leak locations in the Boston area that were detected  
156 using mobile measurements ( $n = 45$ ) in 2011 from Phillips et al. (2013) and additional locations  
157 from later mobile surveys ( $n = 55$ ). They reported  $\text{CH}_4$  emission rates from gas leaks ranging  
158 from  $0.003 \text{ g min}^{-1}$  to  $16 \text{ g min}^{-1}$ , corresponding to roughly  $0.0 - 24.4 \text{ L min}^{-1}$ . They also  
159 reported that their estimate using chamber measurements underestimated total  $\text{CH}_4$  emissions,  
160 likely because the chambers didn't capture the total  $\text{CH}_4$  emitted from the leak. This is similar  
161 to the enclosure measurements results from Weller et al. (2018).

162  
163 The flow through a hole in a pipeline can also be calculated theoretically and empirically from  
164 the physical properties of the hole, mainly the ratio of hole to pipeline diameter and the  
165 overpressure in the pipeline. There are three different engineering model types to estimate  
166 emissions from gas leaks: the hole model, the rupture model and modified models to bridge the  
167 gap between hole and rupture models (Hu et al., 2020; Moloudi and Esfahani, 2014; Yuhua et  
168 al., 2002; Arnaldos et al., 1998). These types of models are either to estimate leak strength from  
169 a pipeline in open space or a buried pipeline. A leak on a buried pipeline has higher surrounding  
170 resistance depending on soil conditions compared to a situation where the pipeline is in open  
171 space. Such models have been used to quantify emissions from holes in pipelines in open space  
172 (Hou et al., 2020; Manda and Morshed, 2017; Moloudi and Esfahani, 2014; Mahgerefteh, Oke  
173 and Atti, 2005; Yuhua et al., 2003; Kayser and Shambaugh, 1991) but also from buried  
174 pipelines (Liu et al., 2021; Ebrahimi-Moghadam et al., 2018; Okamoto and Gomi, 2011; Yan,  
175 Dong and Li, 2015). Cho et al. (2021) introduced a model, which takes into account soil  
176 properties including absolute and relative permeability and porosity, the underground spread  
177 of the leak, surface  $\text{CH}_4$  mole fractions and depth of the buried pipeline based on experiments  
178 with a controlled release rate. This model was calibrated based on release rates ranging from  
179  $1.3 \text{ g min}^{-1}$  to  $5.7 \text{ g min}^{-1}$ , corresponding to roughly  $2.0 - 8.7 \text{ L min}^{-1}$ .

180  
181 In this study, we present results from measurements with the mobile, the tracer release and the  
182 suction methods in Hamburg, Germany, in August and September 2020. We present the  
183 quantitative emission estimates as well as a qualitative intercomparison of the three methods,  
184 in particular related to the applicability and the strengths and weaknesses of the different  
185 methods at different leak locations. We investigate differences between the leaks detected from  
186 mobile measurements and leak locations reported from the routine leak detection surveys  
187 performed by the local gas utility (hereinafter LDC (Local Distribution Company)). Finally,  
188 we discuss implications of our study for national emission inventories.

189

## 190 **2 Materials and Methods**

### 191 **2.1 Campaign preparation and general overview**

192 As a preparation for the intercomparison campaign, all partners contributed to the preparation  
193 of an “intercomparison matrix” where the characteristics and deployment details of the  
194 different methods were specified. This matrix is provided in section S.1 of the Supplemental  
195 Information (SI). The matrix includes descriptions related to the identification of gas leaks, the  
196 quantification of gas leaks, adjustments of the method to the intercomparison exercise and



## 223 **2.2 Measurements setups**

### 224 **2.2.1 Mobile measurement setup**

225 Onboard the measurement vehicle (VW Transporter) we operated two cavity ring-down  
226 spectrometers (CRDS), model G2301 and model G4302 (Picarro, Santa Clara, California,  
227 USA). The G2301 measures CH<sub>4</sub>, CO<sub>2</sub> and water vapor (H<sub>2</sub>O) at a flow rate of  $\approx 0.2 \text{ L min}^{-1}$   
228 and 0.3 Hz frequency. The G4302 has a flow rate of  $\approx 2.2 \text{ L min}^{-1}$  and sampling frequency of  
229 about 1 Hz for CH<sub>4</sub>, C<sub>2</sub>H<sub>6</sub> and H<sub>2</sub>O. The air intake for both instruments was from the same  
230 tubing attached to the front bumper. This setup allowed us to directly compare the  
231 enhancements observed from the two instruments during surveys. The G4302, which is in a  
232 shape of a backpack, was also used in attribution of outlets emissions in walking surveys to  
233 check presence of C<sub>2</sub>H<sub>6</sub> in emission outlets.

234

### 235 **2.2.2 Tracer release measurement setup**

236 The tracer release method was applied by releasing acetylene (C<sub>2</sub>H<sub>2</sub>) at the emission outlet  
237 identified by the mobile leak detection and confirmed by the carpet method. The tracer gas  
238 was released at the main emission outlet, which was confirmed by surface screening using a  
239 handheld CH<sub>4</sub> analyzer. Tracer release rates between 1.3 and 2.6 L min<sup>-1</sup> from a gas cylinder.  
240 A Picarro CRDS, G2203 instrument was used to measure CH<sub>4</sub> and C<sub>2</sub>H<sub>2</sub> mole fractions  
241 continuously with  $\approx 0.3 \text{ Hz}$  frequency. The instrument was installed in a measurement vehicle  
242 (VW Caddy), and air was sampled from the atmosphere through an inlet on the roof about 2m  
243 above ground. The tracer method was applied either in static mode, where air was sampled in  
244 one or a few locations downwind from the outlets and tracer release locations (n = 11) or mobile  
245 mode (n = 5), where the plumes were transected while measuring mixing ratios of CH<sub>4</sub> and  
246 C<sub>2</sub>H<sub>2</sub>. The choice of mode depended on the site conditions including road accessibility and  
247 wind direction. The tracer release setup including instrumentation used as well as mobile mode  
248 is described in detail in Mønster et al (2014), and the principle of the static mode is described  
249 in Fredenslund et al (2010).

250

### 251 **2.2.3 Suction measurement setup**

252 In the suction method, 12 probes were used to insert in the soil around the confirmed gas leak  
253 location by the LDC. The probes are connected to a pump to extract accumulated subsurface  
254 CH<sub>4</sub> from the leak. CH<sub>4</sub> mole fraction at the outflow is measured with a Flame Ionization  
255 Detector (MEEM, 2018).

256

### 257 **2.2.4 Carpet method setup**

258 Leak detection experts from the LDC operate a methane detector (Sewerin instruments,  
259 Gütersloh, Germany) on a rolling device, where a plastic cover (the carpet) moves over the  
260 ground and provides a loose seal to the surrounding atmosphere, facilitating preferential  
261 analysis of air emanating from the surface right below the carpet. The instrument gives an  
262 acoustic signal when a high CH<sub>4</sub> from a potential leak has been detected. The instrument can  
263 detect C<sub>2</sub>H<sub>6</sub> by gas chromatography in batch mode, which means that after taking air samples  
264 from a suspected outlet, the instrument operator needs to wait for couple of minutes to test  
265 possible detection of C<sub>2</sub>H<sub>6</sub>. This is substantially slower than instrument with 1 Hz frequency  
266 used in the mobile method.

267

## 268 **2.3 Detection, confirmation and attribution of emissions at gas leak locations**

### 269 **2.3.1 Mobile detection of possible leak location**

270 For leak detection with the mobile method, we first evaluated CH<sub>4</sub>, C<sub>2</sub>H<sub>6</sub> and CO<sub>2</sub> signals  
271 during mobile surveys. If (i) CH<sub>4</sub> and C<sub>2</sub>H<sub>6</sub> signals were observed with a ratio of less than 10%  
272 with no CO<sub>2</sub> signal or (ii) CH<sub>4</sub> was observed ( $< 500 \text{ ppb}$  enhancement on G4302) with no C<sub>2</sub>H<sub>6</sub>

273 and CO<sub>2</sub> signals, then we parked the mobile measurement car, detached the G4302 analyzer  
274 from the system and searched for gas outlets on foot with the G4302. This detailed search for  
275 outlets was performed to (i) confirm the presence of both CH<sub>4</sub> and C<sub>2</sub>H<sub>6</sub> signals (ii) map the  
276 spatial spread of outlets and (iii) spatially constrain the possible gas leak location. The reported  
277 possible gas leak locations from the mobile method were then reported to the LDC for  
278 confirmation and localization of the leak with the carpet method and subsequent underground  
279 measurements.

280

### 281 **2.3.2 Attribution of leak indication signals from mobile measurements**

282 To attribute an observed leak indication (LI) from mobile measurements to a source category,  
283 namely fossil, microbial and combustion, we used CO<sub>2</sub> and C<sub>2</sub>H<sub>6</sub> signals, which were  
284 continuously measured along with CH<sub>4</sub>. We quantitatively evaluated C<sub>2</sub>:C<sub>1</sub> ratios (%) when (i)  
285 the CH<sub>4</sub> enhancements were larger than 0.5 ppm (ii) C<sub>2</sub>H<sub>6</sub> enhancements were also larger than  
286 15 ppb and (iii) the determination coefficient (R<sup>2</sup>) of the linear regression between CH<sub>4</sub> and  
287 C<sub>2</sub>H<sub>6</sub> was larger than 0.7. If CH<sub>4</sub> signals in mobile measurements were associated with CO<sub>2</sub>  
288 and high C<sub>2</sub>H<sub>6</sub> mole fractions (C<sub>2</sub>:C<sub>1</sub> > 10%), we attributed those emissions to combustion  
289 (Maazallahi et al., 2020). When we repeatedly observed CH<sub>4</sub> enhancements, no CO<sub>2</sub>  
290 enhancements and C<sub>2</sub>:C<sub>1</sub> ratios between 1 and 10%, or we observed persistent CH<sub>4</sub> signals in  
291 several passes we did further on-foot inspection of the outlets. If the emissions from the outlets  
292 clearly pointed to a fossil origin based on the CH<sub>4</sub> and C<sub>2</sub>H<sub>6</sub> signals, we labeled the locations  
293 as potential gas leak locations and reported them to the LDC for confirmation. We only  
294 considered a location as a gas leak for further investigation if the LDC confirmed the existence  
295 of a gas leak.

296 If at a particular location, we observed several CH<sub>4</sub> maxima, for example from different outlets,  
297 we considered the “strongest” outlet as the main emission point. The “strongest” emission point  
298 refers to a point where we observed the highest CH<sub>4</sub> mole fraction when the G4302 intake inlet  
299 was put at a distance of ≈ 2 - 5 cm above the surface or outlet. When several emission outlets  
300 with same order of magnitude in mole fractions were found, we considered the spatial average  
301 of the coordinates as the main emission point. The tracer method then released C<sub>2</sub>H<sub>2</sub> at the  
302 main outlet emission point.

303 The LDC reported a C<sub>2</sub>:C<sub>1</sub> ratio of 3.0% (96.20 ± 0.02 mol % CH<sub>4</sub> and 2.88 ± 0.00 mol %  
304 C<sub>2</sub>H<sub>6</sub>, GNH personal communication) for the gas composition in the grid for the period of  
305 August and September 2020 in Hamburg. This ratio was reported 3.5% (95.09 mol % CH<sub>4</sub> and  
306 3.37 mol %, GNH personal communication) in April 2020.

307

### 308 **2.3.3 LDC leak detection and confirmation**

309 Since the pipeline locations are known to the LDC, the method can be applied precisely above  
310 the pipelines, including visible cracks and cavity outlets in the close vicinity, increasing the  
311 possibility of leak detection. Once the carpet method detects a CH<sub>4</sub> source, a second  
312 measurement is performed above the location with the highest signal, where air is accumulated  
313 and analyzed for the presence of C<sub>2</sub>H<sub>6</sub>. The C<sub>2</sub>H<sub>6</sub> detection in the carpet method is not online  
314 with higher detection threshold and in batch mode (gas chromatography), which takes time, 5  
315 – 10 minutes per location. If sufficiently high CH<sub>4</sub> and C<sub>2</sub>H<sub>6</sub> levels are found, the leak is  
316 categorized in one of safety categories of A1, A2, B or C.

317

### 318 **2.3.4 Precise underground leak localization**

319 When a leak has been confirmed with the carpet method, a precise localization of the leak is  
320 performed by drilling holes about 20-40 cm into the ground along the pipeline track and  
321 measuring the sub-surface CH<sub>4</sub> mixing ratio. The location with the maximum sub-surface  
322 reading is assigned the most likely leak location where the repair teams open the road and

323 attempt repair of the leak. The final exact leak location is reported after opening ground for the  
324 repair reactions. Mostly the locations reported from the carpet method matches the locations  
325 reported from the leak repair team, which depends on the transport pathways of emission  
326 undersurface and surface coverage.

327

## 328 **2.4 Emission quantification**

### 329 **2.4.1 Mobile measurements quantifications**

330 After the detection of the target locations, we performed additional transects at these locations  
331 on different days. We accepted a mobile measurement transect of a leak location for further  
332 analysis if (i) the GPS signals of transects were logged correctly along the street track and (ii)  
333 at least one of the two instruments, G2301 (for quantification and attribution) and / or G4302  
334 (for attribution), were running during the transect and (iii) the transect track included at least  
335 one GPS coordinate less than 50 m from the leak location. The start and end point of the  
336 accepted transects were determined as the locations where the driving tracks intersected with a  
337 circle with radius of 100 m centered at the gas leak location reported by the LDC, or a reported  
338 outlet location from the mobile method, for the locations where the LDC did not confirm a  
339 leak. The segments between the start and end points were evaluated one by one (See an example  
340 in Sect. S.4.1 in SI) to determine various parameters, e.g., the maximum CH<sub>4</sub> enhancements,  
341 plume area, driving speed, distance to the actual leak locations, etc. The plume area is the  
342 integral of the CH<sub>4</sub> enhancements above background along the driving track from the location  
343 where the CH<sub>4</sub> enhancement exceeds > 10 ppb until the location where it falls again below the  
344 10 ppb threshold.

345 Gas leak quantification from mobile measurements is based on an empirical equation derived  
346 from controlled release experiments reported by von Fischer et al., (2017) and reevaluated in  
347 Weller et al., (2019) (Eq. 1).

348

$$349 \quad Q = \exp \left( \overline{\ln (C_{max})} + 0.988 \right) / 0.817 \quad \text{Eq. 1}$$

350

351 In Eq. 1,  $C_{max}$  is the maximum CH<sub>4</sub> enhancement (ppm) observed during each transect next to  
352 the leak location. The maximum CH<sub>4</sub> enhancement should be more than 10% above CH<sub>4</sub>  
353 background level to be considered for the quantification algorithm. The emission rate is  
354 denoted by Q and it is in L min<sup>-1</sup>.  $\overline{\ln (C_{max})}$  is the mean of the logarithm of the maximum  
355 mole fraction enhancements for all accepted transects.

356 The standard quantification method only uses transects where CH<sub>4</sub> enhancements are more  
357 than 10% or  $\approx 200$  ppb above background level. This 10% enhancement threshold corresponds  
358 to about 0.5 L min<sup>-1</sup> emission rate in Eq. 1. Thus,  $\approx 0.5$  L min<sup>-1</sup> is the minimum emission rate  
359 that can be quantified with Eq. 1 and leaks with smaller emission rates are ignored by design  
360 of the method. Below we investigate the effect of relaxing the enhancement threshold. The  
361 application of the tracer release technique in mobile mode allowed us to use the known C<sub>2</sub>H<sub>2</sub>  
362 release rate and the measured C<sub>2</sub>H<sub>2</sub> plumes to independently validate the mobile approach,  
363 including the effect of the enhancement threshold. We also investigated the effect of distance  
364 between CH<sub>4</sub> maxima to gas leak locations, which is not a parameter in Eq. 1.

365 The uncertainty of the emission rate for each location in the mobile method was calculated  
366 using standard error and t-factor (95% confidence) for the locations with at least three CH<sub>4</sub>  
367 enhancements greater than the 10% threshold.

368 In addition to evaluating the maximum CH<sub>4</sub> enhancement from each transect we also derived  
369 the plume area (mixing ratio times distance and in unit of ppm m) for comparison between the  
370 instruments. In principle, the plume area should provide a more robust quantification of an  
371 ambient CH<sub>4</sub> plume than the maximum enhancement: When a plume spreads out, individual  
372 realizations of the plume can be sharper and higher, or wider and lower, depending on



373 meteorological conditions, but the plume area should be less affected. In addition, when an  
 374 instantaneous plume is sampled with two instruments with different gas flow rates, instruments  
 375 with a lower flow rate will be affected by mixing of air in the measurement cell. This will lead  
 376 to a lower maximum enhancement but a wider peak, and thus the peak area should lead to a  
 377 better comparison between the instruments.

378

#### 379 **2.4.2 Tracer measurements quantifications**

380 The tracer method uses Eq. 2a to quantify CH<sub>4</sub> emissions in mobile mode (integral over space  
 381 dimension) and Eq. 2b in the static mode (integral over time dimension). Parameters relevant  
 382 for the evaluation with the tracer method are provided in Sect. S.4.2.

$$383 \quad Q_{CH_4} = Q_{C_2H_2} \cdot \frac{\int_{start}^{end} C_{CH_4} dx}{\int_{start}^{end} C_{C_2H_2} dx} \cdot \frac{MW_{CH_4}}{MW_{C_2H_2}} \quad \text{Eq. 2a}$$

$$384 \quad Q_{CH_4} = Q_{C_2H_2} \cdot \frac{\int_{start}^{end} C_{CH_4} dt}{\int_{start}^{end} C_{C_2H_2} dt} \cdot \frac{MW_{CH_4}}{MW_{C_2H_2}} \quad \text{Eq. 2b}$$

385

386 Here C is the mole fraction (ppm) and MW is the molecular weight of the species, 16 g mol<sup>-1</sup>  
 387 for CH<sub>4</sub> and 26 g mol<sup>-1</sup> for C<sub>2</sub>H<sub>2</sub>.  $Q_{CH_4}$  is the CH<sub>4</sub> emission rate estimate for CH<sub>4</sub> (g s<sup>-1</sup>) and  
 388  $Q_{C_2H_2}$  is the controlled release rate of C<sub>2</sub>H<sub>2</sub> (g s<sup>-1</sup>). The C<sub>2</sub>H<sub>2</sub> flow rate was controlled and  
 389 measured with a flow controller (Brooks Sho-Rate). In addition, the mass of C<sub>2</sub>H<sub>2</sub> released at  
 390 each location was measured by weighing the release cylinder before and after the tracer release  
 391 with a precise scale (KERN DE60K5A). The change in mass was then converted to a mass  
 392 flow rate using the release time. To convert the emission rate from mass (g s<sup>-1</sup>) to volume (L  
 393 min<sup>-1</sup>) we used normal temperature and pressure (NTP) conditions, T = 293.15 K, p = 1.01325  
 394 bar. The locations of tracer release (C<sub>2</sub>H<sub>2</sub>) at the confirmed gas locations were determined with  
 395 the combined information from the mobile and the carpet methods.

396 The tracer gas can also be used to pinpoint and confirm the emission source location. Prior to  
 397 quantification, it is important that the emission outlet is located for proper tracer release (see  
 398 Fig. 1) and source simulation and that other potential interfering emission sources can be ruled  
 399 out. This is secured by performance of upwind and downwind CH<sub>4</sub> mole fraction screening.  
 400 During transecting of the CH<sub>4</sub> and tracer plumes, the two plumes should match, if this is not  
 401 the case, the tracer release should be relocated until a proper plume match is obtained. If an  
 402 emission source consists of multiple outlets, the combined emission from all outlets can be  
 403 measured by releasing the tracer at the main outlet and increasing the measuring distance until  
 404 one confined overlapping plume of CH<sub>4</sub> and tracer gas is obtained. If the distance cannot be  
 405 increased to access limitations, tracer should be released at each single emission outlet.

406

#### 407 **2.4.3 Suction measurements quantifications**

408 The quantification of a leak with suction method is possible after pumping accumulated air out  
 409 of soil and reaching CH<sub>4</sub> mole fraction equilibrium in the outflow. With the equilibrium CH<sub>4</sub>  
 410 reached and the known pumping rate through the probes, it is then possible to calculate  
 411 emission rate (See Sect. S.4.3 in SI).

412

#### 413 **2.4.4 Hole method, based on leak and pipeline properties**

414 The LDC reported the physical properties of gas leaks and pipeline conditions. These include  
 415 leak area, pipeline diameter and pipeline operational pressure. In order to get an estimate of the  
 416 upper physical limits of gas leakage through a hole with the given properties, we used the  
 417 empirical model by Liu et al., (2021), which was designed to quantify emissions from buried

418 natural gas pipelines to estimate emission rates from the leaks (Eq. 3), hereinafter “hole”  
 419 method.

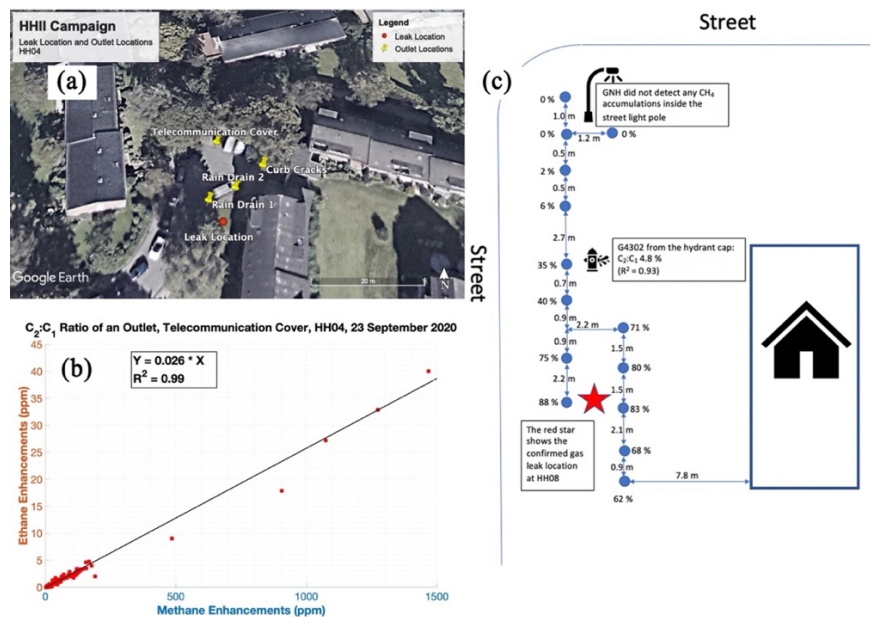
420  
 421 
$$Q = 0.567 \cdot [(h + 139.592)^{-0.1} - 0.542] \cdot d^{1.5} \cdot p^{0.7}$$
 Eq. 3  
 422

423 Here, Q is the gas leak rate in  $\text{m}^3 \text{h}^{-1}$  (at standard atmospheric conditions and converted to  
 424 NTP), h is the depth of the buried pipeline in cm, d is the gas leak hole diameter in mm and p  
 425 is the pipeline overpressure in kPa. We used 150 cm as pipeline depth for all the locations in  
 426 Hamburg to estimate emission rate. We note that the model that we employed is for buried  
 427 pipelines not pipelines in open space, and emission estimates for the gas leak emission rate in  
 428 open space would be even higher (See Sect. 4.4 in SI). Ebrahimi-Moghadam et al. (2018)  
 429 showed that  $\text{CH}_4$  emission from a pipeline hole area can be between 7 to 10 times higher in  
 430 open space relative to the subsurface conditions.  
 431

### 432 3 Results

#### 433 3.1 Leak Detection

435 15 possible leak locations were detected by the mobile method in the initial surveys, (labeled  
 436 as HH001 – HH015). At 13 out of these 15 locations, leaks were confirmed by the LDC, HH007  
 437 and HH012 locations were not confirmed as gas leak locations. In addition, the LDC identified  
 438 5 other leak locations (labeled as HH100 – HH104) that had not yet been fixed (category B and  
 439 C). The overview of the measurements (detection and quantification) is provided in the SI (See  
 440 Sect. S.5 in SI). At some locations we also observed that vegetation was impacted negatively  
 441 by the presence of leaks in their vicinities, a known phenomenon as high levels of methane  
 442 cause harmful anoxic conditions for the plant roots (See Sect. S.6 in SI). At several locations  
 443 the outlet identification was straightforward, because we only observed one outlet, but at 5  
 444 locations we observed numerous outlets spread over a large area. Figure 2 shows the spread of  
 445 emission outlets at one of the locations (Fig. 2a), with correlations of  $\text{CH}_4$  and  $\text{C}_2\text{H}_6$  at the  
 446 “strongest” outlet (Fig 2b). Fig. 2c shows precise gas leak location practice of the LDC at one  
 447 of the other locations.



448  
 449 **Figure 2 – (a) aerial image of location HH004 (© Google Maps). Yellow pins show surface**  
 450 **emission outlet locations, and the red point shows the actual pipeline leak location**

451 reported by the LDC; (b) correlation between CH<sub>4</sub> and C<sub>2</sub>H<sub>6</sub> measured from a  
 452 telecommunication cover; (c) Map (not to scale) of drilled holes (blue dots) to locate the  
 453 pipeline gas leak at HH008. The red star shows the actual pipeline gas leak location as  
 454 indicated by the undersurface CH<sub>4</sub> mole fractions (See Sect. S.3, Fig. S3)  
 455

### 456 3.2 Leak Quantification

457 Table 1 shows the results of the leak emission rate quantifications from the four methods. All  
 458 these locations were quantified by the mobile method, although for 6 of them the 10%  
 459 enhancement threshold was not reached. 16 locations were quantified by the tracer release  
 460 method and 8 by the suction method. A complete overview of key parameters for all  
 461 measurements (detection and quantification) is provided in Sect. S.5.  
 462

463 Table 1 – Results of gas leak quantification with different methods in Hamburg, Germany

	ID	Leak quantification methods (L min <sup>-1</sup> )							Info. from the LDC			
		Mobile (measurements from G2301)			Tracer (L min <sup>-1</sup> )	Suction		Hole (L min <sup>-1</sup> )	Pipeline buried year	Leak size (cm <sup>2</sup> )	Leak type; Safety considerations	Pipeline Size and Material#
		Transect (s) w/ CH <sub>4</sub> Enh. > 10% threshold	Emission average	Emission range; 95% confidence		Emission (L min <sup>-1</sup> )	Status					
Detected by mobile method	HH001	n = 1 (10%)	0.7	-	0.06	<1.8	INC	39	1935	2.5	C	DN80ST
	HH002	n = 5 (50%)	4.9	0.7 – 36.0	0.22	<0.7	INC	45	1935	3.0	A2	DN80ST
	HH003	n = 6 (86%)	7.5	1.1 – 53.0	1.37	-	-	-	1963	-	A1	DN100ST
	HH004	n = 4 (100%)	7.8	1.8 – 34.5	5.33	-	-	-	1959	-	A1	DN80ST
	HH005 <sup>+</sup>	n = 19 (51%)	1.8	0.9 – 3.6	0.21	-	-	-	1935	-	A2	DN80ST
	HH006 <sup>*</sup>	n = 11 (39%)	1.2	0.8 – 1.8	0.02	0.3	CPLT	33	1934	0.5	B	DN80ST
	HH007 <sup>°</sup>	n = 0 (0%)	-	-	-	-	-	-	-	-	-	-
	HH008	n = 6 (26%)	1.5	0.4 – 6.4	0.32	<1.3	INC	-	1934	-	C	DN80ST
	HH009 <sup>×</sup>	n = 9 (38%)	3.9	1.5 – 9.8	4.86	<3	INC	-	1928	-	A1	DN80ST
	HH010	n = 3 (38%)	1.6	0.2 – 13.7	0.51	<0.7	INC	-	1937	-	C	DN200ST
	HH011 <sup>^</sup> ×	n = 4 (50%)	1.9	0.2 – 18.6	0.37	-	-	150	1963	15	A1	DN300ST
	HH012 <sup>°</sup>	n = 0 (0%)	-	-	-	-	-	-	-	-	-	-
	HH013 <sup>^</sup>	n = 2 (40%)	1.8	-	-	-	-	65	1939	5	A1	DN80ST
	HH014	n = 24 (55%)	1.6	1.1 – 2.5	1.41	-	-	65	1950	5	A1	DN100ST
	HH015	n = 1 (50%)	1.0	-	0.38	<0.9	INC	19	1935	1	A1	DN80ST
Reported by the LDC	HH100	n = 1 (13%)	0.7	-	0.14	-	-	-	1994	-	C	d225Pe
	HH101	n = 0 (0%)	-	-	0.07	<0.7	INC	-	1960	-	C	DN80ST
	HH102	n = 0 (0%)	-	-	0.01	-	-	-	1928	-	C	DN125ST
	HH103	n = 0 (0%)	-	-	0.03	-	-	-	1963	-	B	DN150ST
	HH104	n = 0 (0%)	-	-	-	-	-	-	1930	-	C	DN100ST

464 <sup>+</sup> The LDC reported three leak locations, ≈ 30 m distance between the two ends, for this  
 465 location: two leaks with area of 5 cm<sup>2</sup> and one leak with area of 1 cm<sup>2</sup>

466 <sup>\*</sup> Complete measurements for the suction method and used for averaging

467 <sup>^</sup> Leak size reported as sum of total hole area of all the leaks on the pipeline

468 <sup>×</sup> Large difference between leak location and the tracer release location

469 <sup>°</sup> The LDC did not confirm a gas leak

470  
471  
472

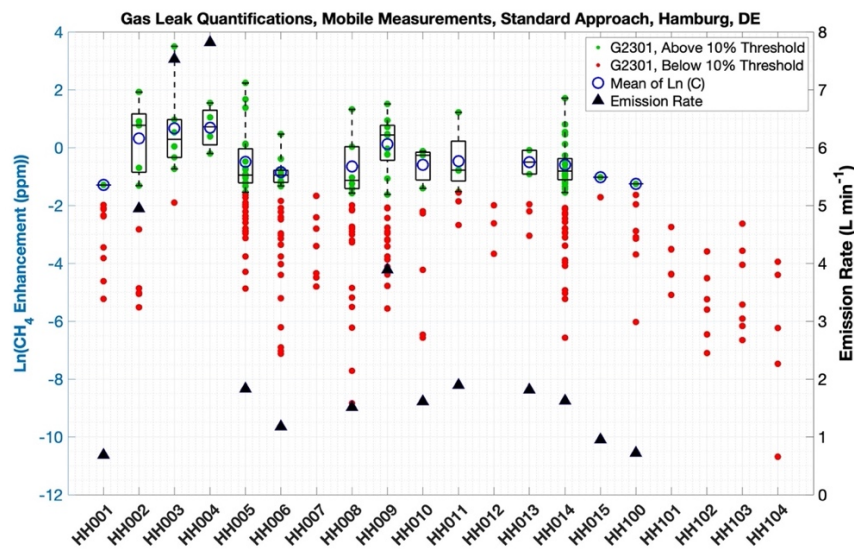
# Pipeline materials, steel (ST) or Polyethylene (Pe), pipeline Diameter Nominal (DN), which is close to the inner pipeline diameter in mm

### 3.2.1 Mobile method

474 The mobile method was applied at all the 20 locations (18 confirmed and 2 unconfirmed gas  
475 leak locations). At 14 (all confirmed gas leak locations) out of the 20 locations, CH<sub>4</sub>  
476 enhancements above the 10% threshold were observed and could be evaluated with the  
477 standard algorithm. The emission rate estimates for these 14 gas leak locations ranged from 0.7  
478 to 7.8 L min<sup>-1</sup>. At the 6 other locations we didn't observe any CH<sub>4</sub> enhancements above the  
479 10% threshold. When we lowered the enhancement threshold to 10 ppb, the emission rates  
480 were 0.07 (HH007; not confirmed gas leak location), 0.1 (HH012; not confirmed gas leak  
481 location), 0.04 (HH101), 0.02 (HH102), 0.05 (HH103) and 0.02 L min<sup>-1</sup> (HH104). Of the 5  
482 leak locations reported by the LDC, 4 did not show any enhancement maximum above the 10%  
483 threshold, i.e., these locations would not have been identified with the default algorithm  
484 (Weller et al., 2018) and would thus not produce an emission estimate.

485 Fig. 2 shows a summary of all individual observed enhancement maxima with the G2301  
486 analyzer from all transects with the mobile vehicle, which were used for the quantification of  
487 emission rates with Eq. 1. The figure illustrates the large spread in enhancement maxima for  
488 multiple passes at each location, similar to Luetschwager et al (2019), leading to large  
489 uncertainties in emission estimates of individual locations. Fig. 2 also shows the diversity of  
490 the various locations, where at some locations most or all of the observed enhancement maxima  
491 are above the 10% threshold (e.g. HH003 and HH004), at several locations none of the  
492 enhancement maxima was above the threshold (e.g. HH101 and HH104) and at other locations  
493 many transects showed enhancement maxima both above and below the threshold (e.g. HH006,  
494 HH008, HH009, HH014).

495 As shown in Fig. 3, there is a wide range of CH<sub>4</sub> enhancement observations per location. This  
496 depends on wind conditions, distance of the observed plume maximum to the emission outlet  
497 location, the superposition of emissions from several outlets and likely other variables such as  
498 soil water content. The mean relative uncertainty from the mean emission rate values for the  
499 mobile method is ≈ 70% for lower and 400% for the upper ends for the locations with at least  
500 3 transects (n = 10) which pass the 10% enhancement threshold (significant signals) in this  
501 study. The lower and upper ranges go down to 60% and 275% for the locations with at least 5  
502 transects (n = 7) with significant CH<sub>4</sub> enhancements.



503  
504  
505

Figure 3 – CH<sub>4</sub> enhancement maxima from all individual transects for each location using G2301. Red points show CH<sub>4</sub> enhancement maxima below the 10% threshold, green

506 points show CH<sub>4</sub> enhancement maxima above the 10% threshold, thus used for the  
507 standard quantification. Blue circles show the  $\overline{\text{Ln}(C_{max})}$  of all the green points for each  
508 location, and black triangles show the derived mean emission rate (based on all green  
509 points) using Eq. 1 for the location with at least one green point (right y-axis).

510

### 511 3.2.2 Tracer method

512 The tracer method performed emission rate quantification at 16 gas locations out of 20  
513 locations. The derived emission rates range from 0.03 to 5.3 L min<sup>-1</sup> (Table 1). For 4 locations  
514 the tracer method was not applied because (i) the emissions were not persistently observable  
515 and the LDC also didn't confirm existence of gas leaks at these locations (n = 2; HH007 and  
516 HH012) or (ii) the leak had already been repaired (n = 1; HH013) or (iii) no emission was  
517 detectable during the visit of the tracer team (n = 1; HH104). For two of the locations (HH11  
518 and HH09), where leaks were confirmed and the tracer method was successfully deployed,  
519 later investigations during repair actions (see Fig. 1) showed that the surface emission outlets  
520 were located far (15 to 60 m) from the actual gas pipeline leak location indicating underground  
521 gas migration. It is evident from Table 2 that the tracer technique can also quantify very small  
522 emission rates, below the cut-off of the mobile technique of 0.5 L min<sup>-1</sup>. Emission rate  
523 estimates derived from the tracer technique were in general lower than the ones derived from  
524 the mobile technique, except for three sites where those were comparable (HH004, HH009 and  
525 H014).

526

### 527 3.2.3 Suction method

528 Due to the time-consuming nature of the suction measurements, initially 10 gas leak locations  
529 had been planned for deployment of the suction method in this campaign. The goal was to  
530 cover a wide range of expected emission rates, as stated in the intercomparison matrix. The  
531 suction method was applied at 8 gas leak locations (see Table 1). At only one location the  
532 quantification could be completed according to protocol where an equilibrium mixing ratio has  
533 to be reached. This was at HH006, with a derived emission rate of 0.3 L min<sup>-1</sup>. At several of  
534 the locations where the mobile method had indicated high emission rates, subsurface  
535 accumulation was widespread, and the suction method was either not deployed (n = 3; HH003,  
536 HH04, HH011) or the measurements were incomplete (n = 7; HH001, HH002, HH008, HH009,  
537 HH010, HH015 and HH101) because of either safety reasons or because the suction team  
538 estimated that they would be unable to complete the measurements within a day. For the 7  
539 locations with incomplete suction measurements, the emission rates were reported ranging  
540 from 0.7 to 3 L min<sup>-1</sup>. These can be regarded as upper limit estimates because suction was not  
541 yet completed and CH<sub>4</sub> mixing ratios would have likely dropped further.

542

### 543 3.2.4 Hole method

544 For 5 locations where the leak area of a single gas pipeline leak was reported, the corresponding  
545 emission rates are between 19 to 65 L min<sup>-1</sup>. For locations HH011 and HH013, the hole area  
546 was reported as the sum of several holes and the total hole area for these two locations resulted  
547 in an emission rate of 150 and 65 L min<sup>-1</sup>, respectively. The quantification from the hole method  
548 is higher than from the mobile, tracer and suction methods by at least an order of magnitude.

549

## 550 3.3 Leak categories

551 The 20 (18 confirmed + 2 not confirmed) locations can be divided into four main categories  
552 related to measurement challenges of the various methods. These categories may overlap.

- 553 (i) Large subsurface CH<sub>4</sub> accumulation
- 554 (ii) Insufficient CH<sub>4</sub> enhancements for mobile quantification
- 555 (iii) Large CH<sub>4</sub> enhancement variability for mobile quantification

556 (iv) Several outlets and / or leaks or atmospheric turbulence

557 In this section we present the overall results and discuss in detail one selected location for each  
558 of these categories. The remaining locations (with similar characteristics) are presented in the  
559 SI.

560

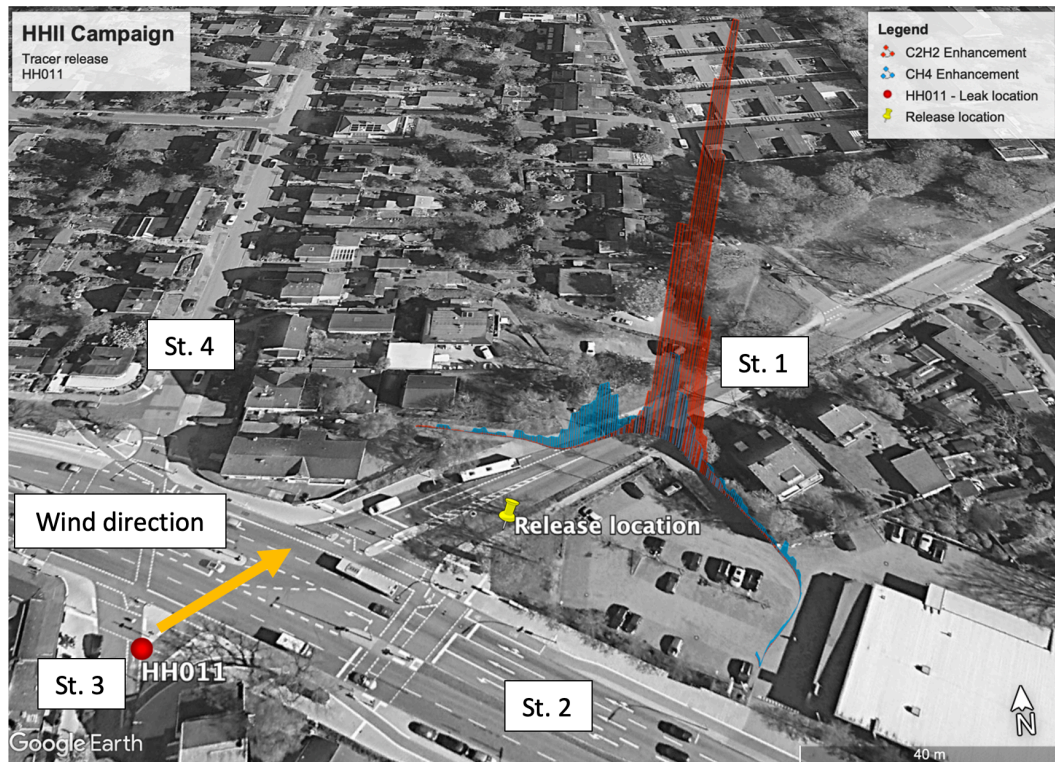
### 561 **3.3.1 Location type I – Large subsurface CH<sub>4</sub> accumulation and multiple outlets**

562 The spatial spread of surface emission outlet locations identified with the G4302 instrument as  
563 part of the mobile method provides an indicator for the extent of the subsurface accumulation  
564 of CH<sub>4</sub>. For 5 locations, emission outlets were found at great distance from each other, in order  
565 of tens of meters. The total emission of a gas leak is equal to the sum of emissions from all the  
566 surface outlets at a location, thus it is necessary to quantify each outlet separately to get the  
567 total emission.

568 HH011 (Fig. 4) is an example where very widespread CH<sub>4</sub> accumulation and migration was  
569 observed. During the initial mobile gas leak detection, leaks were located at the intersection of  
570 streets 1 and 2, close to a subsurface vent and a rain drain,  $\approx$  2 m apart, (the yellow pin in Fig.  
571 4a) based on clear signals from these outlets and a sign next to the road indicating presence of  
572 gas pipelines. The vent showed a C<sub>2</sub>:C<sub>1</sub> ratio of 2% (R<sup>2</sup> of 0.8 and max CH<sub>4</sub> mole fraction of  
573 31 ppm) and we observed C<sub>2</sub>:C<sub>1</sub> ratio of 2.8% with R<sup>2</sup> of 0.96 and max CH<sub>4</sub> mole fraction of  $\approx$   
574 70 ppm from the rain drain, clearly indicating a large / dominant contribution from fossil CH<sub>4</sub>.  
575 However, after quantifying the emission from these two leaks using the mobile and the tracer  
576 release methods, the LDC found the actual gas pipeline leak, during the repair actions, on the  
577 south side of the intersection, far from the vent and the rain drain, at the intersection of street  
578 no. 3 and no. 2 indicating that the gas had travelled about 60 m underground. It is possible that  
579 the leak resulted in several gas emission outlets, likely closer to the gas pipeline leak location.  
580 The emission rate measured using the mobile method was 1.6 L min<sup>-1</sup> based on 5 plume  
581 transects and is likely underestimated because some emission outlets potentially were not  
582 included in the performed plume transect. It should also be noted that the distance from the gas  
583 pipeline leak location to the plume transect is larger than the distances applied during the  
584 controlled release calibrations (average 15 m) (Weller et al., 2019).

585 The tracer was released at the vent and the rain drain and thus measured the combined emission  
586 from these two outlets to be 0.4 L min<sup>-1</sup>. If the gas pipeline leak gave rise to multiple  
587 unidentified surface emission outlets, the emission from the gas pipeline is underestimated. IN  
588 fact, Fig. 4b shows that a CH<sub>4</sub> plume without C<sub>2</sub>H<sub>2</sub> was observed during the tracer release  
589 measurements at HH011, confirming that at least one other source of methane emission was  
590 present nearby.

591 Based on the previous experience at locations with widespread subsurface accumulation it was  
592 concluded that the suction method could not be applied at this location. The other case in this  
593 category was HH009.



594

595

596

597

598

599

600

601

602

603

604

605

606

607

608

609

610

611

612

613

614

615

616

617

618

619

620

621

622

623

**Figure 4 – aerial image of HH011 (© Google Maps). A gas leak location with widespread undersurface CH<sub>4</sub> accumulation. The yellow pin shows the assumed leak location and location of tracer release, which was very different from the actual leak location as identified by the LDC (red circle). St. 1-4 are added to identify streets that are discussed in the text. General wind direction during tracer release deployment is shown with an orange arrow. CH<sub>4</sub> (in blue) and C<sub>2</sub>H<sub>2</sub> (in red) levels measured at a plume transect. One of the CH<sub>4</sub> plume is proportional to the C<sub>2</sub>H<sub>2</sub> plume while the other CH<sub>4</sub> plume lacks the C<sub>2</sub>H<sub>2</sub> signals suggesting existence of at least another emission outlet.**

The LDC reported the total area of several holes in the pipeline as 15 cm<sup>2</sup> for HH011, which is the largest leak size among all the locations. If we assume that there was one hole with this size, then the emission rate estimated by Eq. 3 will be 150 L min<sup>-1</sup>, a hole of 5 cm<sup>2</sup> gives emission rate of 65 L min<sup>-1</sup>. The pipeline for this location was DN300ST and has been in operation since 1963.

### 3.3.2 Location type II – Insufficient CH<sub>4</sub> enhancements for mobile quantification

At HH101, on a narrow ( $\approx 3$  m wide) street, which had about 1 m wide bare soil pavement on one side, the LDC reported a gas leak location based on their routine surveys. On both sides of the street there were about  $\approx 1.5$  m tall bushes and some trees. All three methods (mobile, tracer and suction method) were deployed at this location. Gas emissions found their way to the atmosphere through cracks in the asphalt with C<sub>2</sub>:C<sub>1</sub> ratio of 2.5% (R<sup>2</sup> of 0.93) with max CH<sub>4</sub> mole fraction of  $\approx 25$  ppm. None of the CH<sub>4</sub> enhancement maxima observed during the mobile surveys at this location were above the 10% enhancement threshold with the G2301 instrument, thus this location would not be labeled as LI and no quantification would be reported from mobile method as implemented in Weller et al (2019) and Maazallahi et al. (2020). The tracer method was applied in static mode at a distance of  $\approx 15$  m and reported an emission rate of 0.1 L min<sup>-1</sup>, which is compatible with the emission strength being below the “detection limit” defined by the 10% cut-off of the standard algorithm (0.5 L min<sup>-1</sup>). When the emission strength is evaluated using the CH<sub>4</sub> enhancements below the cut-off, the value is 0.04 L min<sup>-1</sup>. The

624 suction method was applied at this location but an equilibrium was not achieved after 9 hr, i.e.  
625 incomplete suction measurements, and an upper limit for the emission rate of  $\approx 0.7 \text{ L min}^{-1}$  was  
626 reported. The fact that the suction measurement was incomplete at this location with a small  
627 emission rate shows that subsurface accumulation can also be large for smaller leaks.

628 Three of the leak locations in this study only showed one  $\text{CH}_4$  enhancement above threshold.  
629 The 10% threshold is a constraint, which removes enhancements less than about 200 ppb. This  
630 means for the locations where we only have one transect with  $\text{CH}_4$  enhancements more than  
631 the 10% threshold, the minimum emission rate estimated is about  $0.5 \text{ L min}^{-1}$ , no matter how  
632 many transects we had with  $\text{CH}_4$  enhancements less than the 10% threshold. This situation was  
633 observed for HH001, HH015 and HH100 (Fig. 5). In this case, the mobile method likely  
634 overestimates the total leak rate, because only the maximum enhancement is used for  
635 quantification. The tracer method reported low emission rates for these three sites  $0.12 \text{ L min}^{-1}$   
636 on average ( $n = 6$ ).

637 For the two locations (HH007 and HH012) where the LDC didn't confirm gas leaks (despite  
638 periodic observation of  $\text{C}_2\text{H}_6$  at outlets during the mobile surveys) none of the transects showed  
639  $\text{CH}_4$  enhancement maxima above the 10% threshold. At HH007, the outlet was through cracks  
640 in the pavement but at HH012 the outlets were from manholes. At HH007 the outlet location  
641 had shifted by about 2 m for two different days (4-week gap). We note that the correlation  
642 coefficients between  $\text{CH}_4$  and  $\text{C}_2\text{H}_6$  at these locations were between 0.4 and 0.6, so less than  
643 0.7, which is the threshold correlation we accepted for the outlets. As a leak was not confirmed  
644 for these locations, the tracer and suction methods were not applied.

645

### 646 **3.3.3 Location type III – Large $\text{CH}_4$ enhancement variability for mobile quantification**

647 For several locations, we observed a large variability of  $\text{CH}_4$  enhancements from different  
648 transects. One example is HH008, where only 6 of the 23 transects exceeded the 10% threshold,  
649 i.e. the leak was only observed in about every 4<sup>th</sup> transect. The leak location of HH008 is an  
650 example where  $\text{CH}_4$  enhancements from several transects cover a wide range. Based on the 6  
651 transects, which showed enhancement maxima above the 10% threshold, a leak rate of  $1.5 \text{ L}$   
652  $\text{min}^{-1}$  is derived. This may be an overestimate since many transects with maxima below the  
653 threshold were not considered. For this location the mobile tracer method was applied, which  
654 resulted in a leak rate quantification of  $0.3 \text{ L min}^{-1}$ .

655 The suction method derived an upper emission estimate of  $1.3 \text{ L min}^{-1}$  from incomplete  
656 measurements at HH008. The LDC reported a C category leak for this location from a DN80ST  
657 pipeline, which was installed in 1934.

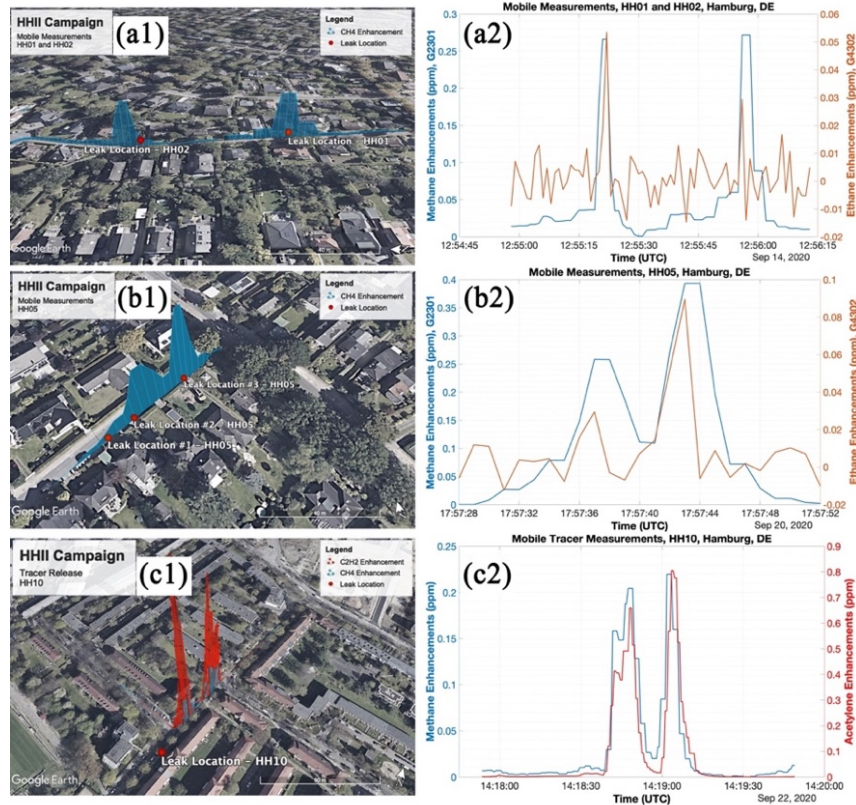
658

### 659 **3.3.4 Location type IV – Several outlets and / or leaks or atmospheric turbulence**

660 On a  $\approx 5 \text{ m}$  wide street, we detected two leaks about 80 m away from each other, HH001 and  
661 HH002 (Fig. 5a). It was a cobblestone street and there were bushes and few trees planted,  
662 mostly on one side of the street. The mobile method performed 10 transects at both locations  
663 and all the transects were accepted for the evaluation. The tracer team could quantify both  
664 locations using static measurements. The suction team began to quantify HH002 and HH001,  
665 but during quantification of HH001, there was a small accident (fire due to contact of drilling  
666 head with electric cable) and the leak had to be fixed immediately. The plumes on this street  
667 were sufficiently separated to positively identify two different leaks on the same street. In  
668 contrast, at location HH005, we observed several maxima for the same transect, but because  
669 the maxima were close to each other, those were clustered together in the mobile measurement  
670 algorithm (Fig. 5b). Later the LDC reported even three individual pipeline leaks on this street.  
671 In another example (HH010), some transects showed several plume maxima although only one  
672 emission outlet and later on only one gas pipeline leak was found (Fig. 5c). However, the  
673 release of the tracer resulted in several matching  $\text{CH}_4$  and tracer gas plumes confirming that



674 the emission indeed occurred from a single outlet and that the multiple plumes at this location  
 675 were due to inhomogeneous plume dispersion. This illustrates that the existence of several  
 676 maxima in one transect does not necessarily correspond to presence of several leaks and/or  
 677 outlets, but it can also be related to a spatially heterogeneous/disturbed plume. This shows that  
 678 the signals from the mobile detection method are not sufficient to allow determining the  
 679 number of leaks at a location with several plume at a close distance from each other in a single  
 680 transect.  
 681



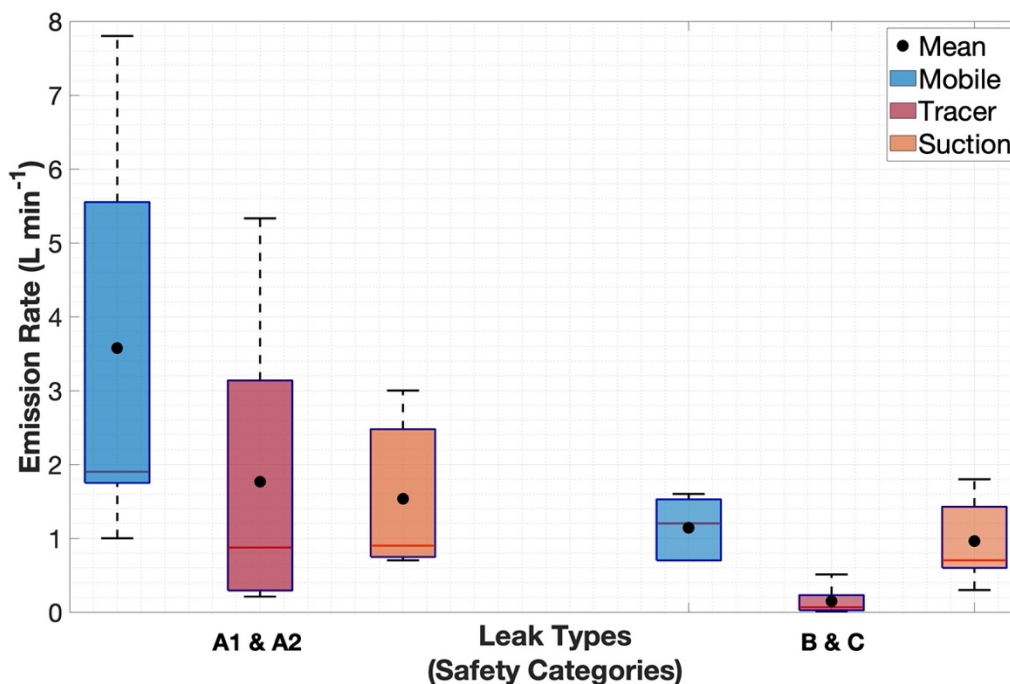
682  
 683 **Figure 5 - Several maxima observed during a single transect on one street showing**  
 684 **different situations: two well isolated leaks with about 80 m distance from each other (a1**  
 685 **and a2, HH001 and HH002), three pipeline leaks close to each other with several emission**  
 686 **outlets (b1 and b2, HH005) and one leak and one outlet but several CH<sub>4</sub> enhancement**  
 687 **maxima due to turbulence (c1 and c2, HH10), aerial images: © Google Maps.**  
 688

689 After detection by mobile measurements, emissions out of the ground were detected at HH001  
 690 and HH002 with the G4302 backpack within 3 m distance from the gas pipeline leak locations,  
 691 which was later reported by the LDC. For the single transect with a maximum above the 10%  
 692 threshold observed with the mobile method, the derived emission rate at HH001 was 0.8 L min<sup>-1</sup>  
 693 (n = 1). For HH002, the derived emission estimate for the transects with maxima above the  
 694 threshold is 5.2 L min<sup>-1</sup> (n = 5) from the mobile method. At HH002, individual derivation of  
 695 emission from separate CH<sub>4</sub> enhancement gives a wide range between 0.7 and 36.0 L min<sup>-1</sup>  
 696 (95% confidence) from the mobile method (see category III above). For HH001, the tracer  
 697 method was applied in static mode at ≈ 30 m distance to the release point and ≈ 40 m far from  
 698 HH002. The derived emission rate for HH001 is 0.06 L min<sup>-1</sup> and for HH002 0.22 L min<sup>-1</sup> from  
 699 the tracer method. For HH001, after about 5 hr of pumping, the suction quantification had to  
 700 be stopped due to the incident described above. Based on the incomplete suction measurement  
 701 an upper limit for emission rate of ≈ 1.8 L min<sup>-1</sup> for HH01 was estimated. An emission estimate  
 702 of ≈ 0.7 L min<sup>-1</sup> was derived for HH002 from an incomplete suction measurement. The LDC

703 reported leak size of  $\approx 2.5 \text{ cm}^2$  for HH001 and for  $\approx 3 \text{ cm}^2$  for HH002 which then give emission  
 704 rate of 39 and 45  $\text{L min}^{-1}$  respectively from the hole method. For both locations, leaks were due  
 705 to pipeline corrosion.  
 706

### 707 3.4 Emission rates of different leak safety types

708 The 18 confirmed gas leak locations that were investigated in the campaign were categorized  
 709 into the four safety categories, A1 ( $n = 7$ ), A2 ( $n = 2$ ), B ( $n = 2$ ) and C ( $n = 7$ ). The mobile  
 710 method quantified all the A1 and A2 leaks ( $n = 9$ ) with an average emission rate of 3.6  $\text{L min}^{-1}$ .  
 711 5 out of 9 leaks in categories of B and C leaks were quantified with the mobile technique  
 712 including the 10% threshold with average emission rate of 1.1  $\text{L min}^{-1}$  ( $n = 5$ ). Apart from one  
 713 location, which had to be fixed before the measurements, the tracer method quantified the A1  
 714 and A2 leaks ( $n = 8$ ) and reported an average emission rate of 1.8  $\text{L min}^{-1}$ . The tracer method  
 715 also quantified all the B and C leaks ( $n = 9$ ) with an average emission rate of 0.1  $\text{L min}^{-1}$ .  
 716 Mostly due to the safety and time constraints and medium to large underground accumulations  
 717 of  $\text{CH}_4$ , the suction method could provide incomplete measurements at only 3 locations of A1  
 718 and A2 leaks with an average emission rate of 1.5  $\text{L min}^{-1}$  ( $n = 3$ ). The suction method measured  
 719 at 5 out of 9 B and C locations, one of the measurements was complete and the others were  
 720 incomplete, with an average emission rate of 1.0  $\text{L min}^{-1}$  ( $n = 5$ ). Although the number of  
 721 quantified leaks is limited, all the three methods show that the emission rates from category A1  
 722 and A2 leaks are higher than category B and C leaks (Fig. 6). This indicates that the site  
 723 selection bias of measurements for the suction method due to safety concerns (see qualifier  
 724 above), can lead to a bias in the emission rate in this method. Except for three leaks (HH003,  
 725 HH009 and HH011), leaks were located by the repair team where the carpet method reported.  
 726 These three leaks were finally found at some distance from the location initially indicated by  
 727 the carpet method. These three leaks are medium or high emitters and belong to type A1.  
 728 Although the number of locations in this study is very small, this supports the common sense  
 729 assumption that bigger leaks can spread out more widely in soil and contaminate larger  
 730 undersurface area. Therefore, the bigger leaks may be mislocated by the carpet method, and  
 731 they are also more likely to fill cavities, placing them in a higher safety category.



732 **Figure 6 – Emission rate differences between different gas leak safety categories.**  
 733

## 4 Discussion

### 4.1 Leak detection methods

#### 4.1.1 Leak location vs outlet location

There is a difference between the location of the leak in the gas pipeline (leak location; See Sect. S.7 in SI) and the location where the gas is emitted to the atmosphere (outlet locations; See Sect. S.2 in SI). Furthermore, a single leak in the gas pipeline can result in multiple emission outlets at the surface. In this campaign we observed that in most cases (2 out of 18), the emission outlet at the surface occurred only a few m (sometimes < 1 m) from the location of the leak in the gas pipeline. However, in one case, an emission outlet was detected about 60 m away from the leak location indicating significant underground gas accumulation and migration (see Fig. 4).

#### 4.1.2 Intercomparison of the gas leak detection methods

The mobile method detects atmospheric CH<sub>4</sub> enhancements while measuring continuously with ppb precision from an inlet installed at the front bumper of the car while LDCs apply the carpet method with an instrument precision at the ppm level. High precision for the carpet method is not needed as the inlet to their instruments is connected to a carpet, which is attached to the ground. The mobile method can cover larger areas in shorter times, but not all roads, walkways, or other surface areas where pipelines are buried are accessible with a vehicle. The advantage of the carpet method is that it can precisely follow the pipeline map, which also means that it can locate leaks more precisely. The mobile method uses a 10% threshold to neglect unreliable gas leak sources, which sometimes results in neglecting actual signals from small leaks. Also the mobile measurements do not detect all leaks due to the dependence on the wind direction (only downwind sources leaks can be detected). Luetschwager et al. (2021) suggested that 5 to 8 plume transects give > 90% probability of gas leak detection at a given location, so if all the streets in an urban area are covered 5 to 8 times, > 90% of the leaks can be detected by mobile measurements.

Both the mobile and the carpet method use C<sub>2</sub>H<sub>6</sub> signals for distinguishing between fossil and microbial CH<sub>4</sub> emissions, and as for C<sub>2</sub>H<sub>6</sub>, the instrument used in the mobile method is more sensitive, and faster. In the carpet method, the laboratory analysis of C<sub>2</sub>H<sub>6</sub> is slow and with higher detection threshold compared to the mobile method, where C<sub>2</sub>H<sub>6</sub> is measured in real-time during the surveys, and also on foot from the emission outlet. The CRDS instrument provides real-time measurements of CH<sub>4</sub> and C<sub>2</sub>H<sub>6</sub> at 1 Hz frequency so checking various outlets at a possible gas leak location is faster.

At 14 out of the 20 locations in this study, gas leaks were detected (CH<sub>4</sub> signals passing the 10% threshold) and quantified with the mobile method. However, we observed that 4 out of 5 locations reported by the LDC would not have been detected in mobile surveys without prior information on existence of the leaks because the maximum enhancement was below the mobile detection threshold. At the only location (HH100) from the list of the LDC, where mobile method could quantify the emissions, the outlets were located on the road and the vehicle was driving on top of the outlet. For this location only one of the transects passed the 10% enhancement threshold, and the quantification for this location was  $\approx 0.7 \text{ L min}^{-1}$ , close to the detection threshold of this method,  $\approx 0.5 \text{ L min}^{-1}$ . One of the other locations, HH101, reported by the LDC had similar surrounding conditions (e.g. presence of buildings, road conditions, etc.) as the other leaks detected by the mobile method, but still the mobile method was not able to detect a gas leak at this location without a priori information from the utility. The quantifications made by the tracer method suggest that the emission rates of the locations provided by the LDC were much lower than the locations detected by mobile measurements

782 (Table 1). The 10% threshold in the mobile method precludes the identification of small leaks  
783 ( $< 0.5 \text{ L min}^{-1}$ ), which would only be identified by the carpet method.

784

## 785 **4.2 Signal attribution in mobile detection method**

### 786 **4.2.1 Attribution during mobile survey in car**

787 During the mobile measurements we used two approaches to find correlation between  $\text{CH}_4$  and  
788  $\text{C}_2\text{H}_6$ . When we compare the online measurements point by point, the probability of detecting  
789 a fossil signal is high, as only one single significant reading is sufficient to indicate a fossil  
790 signal. When we use the  $R^2$  of the linear correlation between  $\text{CH}_4$  and  $\text{C}_2\text{H}_6$  enhancements  
791 above the cut-off, the attribution is more reliable. In a large dataset without a priori information  
792 on the existence of a gas leak at different locations, the correlation method is more trustworthy  
793 as the point-by-point method could be affected by instrument noise and/or spikes.

794 We also used  $\text{CO}_2$  signals and their correlation with  $\text{CH}_4$  signals to investigate interference  
795 from combustion or microbial processes. For only 7 plumes at 6 locations, we detected  
796 correlations between  $\text{CO}_2$  and  $\text{CH}_4$ , which could indicate either oxidation of  $\text{CH}_4$  to  $\text{CO}_2$  or  
797 mixture of microbial  $\text{CH}_4$  emissions from e.g. the sewer system with the emissions from natural  
798 gas leaks. The number of these possible co-emissions is low compared to the number of total  
799 transects (only  $\approx 7\%$  of the plumes with  $\text{CH}_4$  enhancements greater than 10%), thus such an  
800 admixture of microbial  $\text{CH}_4$  should not impact the quantification from mobile method  
801 significantly.

802

### 803 **4.2.2 Plume attribution to emission outlets**

804 The outlet attribution was performed using the G4302 CRDS instrument which is portable like  
805 a backpack. We checked the outlets (See Sect. S.2, Fig. S1) around the locations of interest and  
806 evaluated the correlation between  $\text{CH}_4$  and  $\text{C}_2\text{H}_6$  and the persistence of the emissions on  
807 different days. In theory, it is possible to estimate contributions of fossil and microbial  $\text{CH}_4$  in  
808 a plume using the ethane signals during the mobile measurements with the vehicle and the  
809 reference  $\text{C}_2:\text{C}_1$  ratio provided by the LDC. However, due to the low  $\text{C}_2\text{H}_6$  signals in ambient  
810 air, it was not feasible to quantify the possible contribution of microbial methane emissions.  
811 Nevertheless, the  $\text{C}_2\text{H}_6$  signals of the G4302 CRDS instrument were still very useful to identify  
812 a location as a possible gas leak location or not. For all the 15 locations, which were initially  
813 detected by the mobile method we observed detectable  $\text{C}_2\text{H}_6$  signals, including the two  
814 locations which later were not confirmed as a gas leak location by the LDC. This suggests that  
815 either the leak is at a greater distance and depending on the transport of the emission we  
816 periodically can see the signals at the detected outlets or that there are sources that produce  
817 both  $\text{CH}_4$  and  $\text{C}_2\text{H}_6$  in the vicinity of the location.

818

## 819 **4.3 Leak quantification methods**

### 820 **4.3.1 Mobile method**

821 If the outlets are close to each other, we may observe several  $\text{CH}_4$  enhancements close to each  
822 other or overlapping when a single transect is performed at a close distance. If we assume that  
823 the number of  $\text{CH}_4$  maxima is equivalent to the number of real outlets that exist on a road and  
824 only use the maximum enhancements from the most pronounced plume to calculate the  
825 emission rate, the total emission will be underestimated with the mobile method.

826 Emission rate estimates with the mobile method from individual transects are associated with  
827 high uncertainty, related to variabilities in either above-ground or under-ground conditions. For  
828 example, an unfavorable wind direction (above ground condition) can result in missing a plume  
829 from a gas leak. The mobile measurement van itself may also affect the measurement, e.g., by  
830 creating pressure fluctuations. Luetschwager et al. (2021) showed that the quantifications from  
831 the same leak in individual mobile transects can vary by more than an order of magnitude. In

832 Hamburg, we found that the range can be even a factor 50 or 100 in exceptional cases (Table  
833 2). This high variability illustrates that if we perform only one transect per location, the  
834 estimated leak emission rate can result in high under / overestimation in emission estimate for  
835 the single location, as was also reported by Maazallahi et al. (2020). This large uncertainty for  
836 individual locations is less severe when the results are extrapolated to the city-level, where the  
837 sample size is also large, including over- and underestimates (Brandt et al., 2016).

838 In our previous study in Hamburg (Maazallahi et al., 2020) the overall average emission rate  
839 for all the LIs was estimated  $3.4 \text{ L min}^{-1} \text{ LI}^{-1}$  ( $n = 145$ ) while for the fossil-attributed  
840 locations it was  $5.2 \text{ L min}^{-1} \text{ LI}^{-1}$  ( $n = 45$ ; standard error of 3.1). This showed that the biggest  
841 emitters were among the fossil categories. In the present study, the average emission rate from  
842 mobile measurements for the gas leak locations is  $2.7 \text{ L min}^{-1} \text{ LI}^{-1}$  ( $n = 14$ ; standard error of  
843 0.6). The higher average emission rate per fossil location in the first campaign may have been  
844 caused by the fact that in that campaign only a smaller number of transects were performed per  
845 location (on average 1.1 in the previous study versus 6.9 transects with  $\text{CH}_4 > 10\%$  threshold  
846 per location in the present study). Luetschwager et al. (2021) stated that after 6 transects with  
847  $\text{CH}_4$  exceeding the 10% threshold per location the average overestimation of leak size estimates  
848 will be less than 10%. In addition, the differences in sample size and locations in these two  
849 studies (45 versus 14 locations in the first and second studies respectively) may partially  
850 explain the difference in average. This is because the probability of detecting large emitters,  
851 which increase the average emission rate of all leaks, increases with sample size.

852 The two  $\text{CH}_4$  sensors onboard the mobile van play specific roles in the detection and  
853 quantification of leaks.  $\text{CH}_4$  enhancements on the G2301 are 3.8 times lower than the G4302.  
854 This is an artefact of the G2301, which smoothes the signal compared to the G4302 because of  
855 the slower pump and sampling rate (See Sect. S.8.1 in SI). On the other hand, this results in  
856 more signals passing the 10% threshold on G4302. This then also leads to higher detection  
857 probabilities using G4302 (See Sect. S.8.2 in SI). Higher record of  $\text{CH}_4$  enhancements also  
858 results in higher emission rate quantification using Eq. 1 (See Sect. S.8.3 in SI). We use the  
859 G2301 for quantification, since this is the instrument that was also used for introduction of the  
860 mobile equation quantification in Weller et al. (2017). The quantification of the gas leak  
861 locations using Eq. 1 depends only on the  $\text{CH}_4$  enhancements. This gives about a factor 2 higher  
862 emission rates from G4302 than from G2301 for the same plumes. When we evaluate the plume  
863 areas from the two instruments, they are much closer to the 1:1 line (See Sect. S.8.3 in SI). This  
864 agrees with findings from another study using two different in-situ instruments onboard a  
865 mobile car (See Sect. S1.5, Fig. S6 from Ars et al. (2020)). They also found that the plume area  
866 is closer to the 1:1 line in mobile measurements even if the air intakes are not at the same  
867 location of the vehicle. This suggests that the plume area is a more robust parameter than  
868 maximum enhancement for emission rate quantification and a leak rate quantification equation  
869 using the plume area should be developed.

870 In general, the closer the air intake is to the emission point the higher the  $\text{CH}_4$  mole fraction  
871 reading is (See Sect. S.9 in SI), but when several outlets are present at one location it is not  
872 possible to uniquely determine the distance to the emission point, and also determine which  
873 plume belongs to which outlet. Eq. 1 from Weller et al. (2019) only uses the maximum  $\text{CH}_4$   
874 enhancements above the 10% threshold from each pass. In their controlled release experiments  
875 the average distance between the leak and measurement was 15.75 m. Analysis of our results  
876 (Table S4, Sect S.5 in SI) shows that higher maximum mixing ratios are encountered more  
877 often when the distances of the transect to the leak location are small. For example, at HH002  
878 the transect was very close to the main emission point, which likely leads to the substantially  
879 higher emission rate estimate derived from the mobile method ( $4.9 \text{ L min}^{-1}$ ) compared to the  
880 tracer method ( $0.22 \text{ L min}^{-1}$ ). On the other hand, at HH011 the mobile method underestimates  
881 the emission rate (See Sect. 3.3.1), as at this location the measurement distance to the leak was

882 larger than reference distance of 15.75 m applied by Weller et al. (2019). This suggests that to  
883 reduce the quantification error for individual leak locations, distance should also be included  
884 in an improved transfer equation. Although distance is a parameter in some quantification  
885 methods, e.g. gaussian plume dispersion, and not in others, e.g. in mass balance, to the best of  
886 our knowledge, this is the first study providing field evidence that distance is a factor that can  
887 affect emission quantification using the Weller et al. (2019) method.

888 The effect of neglecting or retaining the transects with enhancement maxima below the 10%  
889 threshold was quantitatively investigated for 5 locations where the tracer team conducted  
890 mobile measurements (See Sect. S.10 in SI). These measurements were evaluated as  
891 “controlled release” experiments for  $C_2H_2$ , because the actual  $C_2H_2$  release rate is known, and  
892 measurements were made in mobile mode. The standard mobile quantification algorithm with  
893 the 10% threshold yields emission estimates that are in relatively good agreement with the  
894 released quantities, whereas the estimates are biased considerably low when measurements  
895 with maxima below the threshold are retained. This supports the use of the original method,  
896 which removes transects with an improper realization of the plume. Relating to section 4.5, it  
897 must be noted, however that in these measurements the distances of the  $C_2H_2$  maxima to the  
898 release points were between 30 to 45 m, thus larger than the normal distance of mobile  $CH_4$   
899 measurement to the emission outlets (from few meters up to 30 m).

900

#### 901 **4.3.2 Tracer method**

902 The tracer method is more labor intensive than the mobile method. However, the strength of  
903 the method is the application of a tracer gas providing the plume dilution and avoiding the use  
904 of atmospheric dispersion models and weather information. If the tracer release location does  
905 not reflect the sum of all the outlet emissions at a gas leak location, or misses some of the  
906 outlets, then the total emission quantification from the gas leaks will be underestimated. An  
907 example of such a case is site HH011 in this study where the leak location in the gas pipeline  
908 (after quantification; see Fig. 1) was found to be located about 60 m upwind the targeted  
909 emission outlet. During tracer quantification, an additional  $CH_4$  plume (not defined by the  
910 tracer gas) was observed indicating more than one emission outlet (Fig. 4). The confirmation  
911 for this is the finding of gas leak location by the carpet method. The emission rate of the  
912 targeted emission source (the vent and the drain) is thus not representing the combined  
913 emission from the gas leak in the pipeline located 60 m upwind the emission source. Further  
914 surface screening and leak detection would have been needed to identify and quantify all  
915 emission outlets.

916

#### 917 **4.3.3 Suction method**

918 The suction method is the most labor-intensive quantification method. Following a strict, safety  
919 first, protocol the gas utilities fix leaks in the A1 safety category immediately upon detection  
920 and A2 leaks within a week. Given logistical constraints, the suction method therefore mainly  
921 or exclusively quantifies B or C leaks (50% of confirmed gas leak location in this study). We  
922 investigated whether such a site selection bias could lead to a bias in the average quantified  
923 emission rate in the inventory report. In this study, we observed that the leaks detected from  
924 the mobile methods were mostly in the A1 and A2 category and the biggest emitters (based on  
925 the mobile and tracer release measurements) had soil  $CH_4$  accumulation of a magnitude that  
926 prevented successful application of the suction method. Further research is needed to identify  
927 the physical mechanism(s) to explain the observed correlation between A1 and A2 leaks and  
928 high emission rates. As a hypothesis, the presence of soil cavities associated with leak category  
929 A1 may result in higher permeability, i.e. lower underground resistance, which then leads to  
930 higher emission rate for the same pipeline hole size compared to locations with no cavity.

931 The suction method was intended to be deployed right before the repair actions. For some of  
932 these locations, the suction method was in operation for more than 10 hours, but due to the high  
933 soil CH<sub>4</sub> accumulation, the measurements were stopped and labeled as incomplete in this study.  
934 For the other locations with high soil CH<sub>4</sub> accumulation, the suction method was not attempted,  
935 given the expectation (based on experience at the incomplete locations) that completion of  
936 measurements for leak rate quantification at those locations was unlikely.

937

#### 938 **4.3.4 Hole method**

939 Based on the leak size, pipeline depth and overpressure, the average emission rate was  
940 estimated at 40 L min<sup>-1</sup> (n = 5). We note that these estimated should be regarded as upper limits  
941 since flow restrictions outside the pipe are not included. The emission range of individual gas  
942 leaks based on the hole method is between 19 to 150 L min<sup>-1</sup> for 1 cm<sup>2</sup> to 15 cm<sup>2</sup> hole sizes  
943 respectively, larger than any of the measurement-based quantification methods. This method  
944 requires information about the overpressure of the gas pipeline, depth of buried pipeline and  
945 size of a leak and it does not include the information about soil properties, which can impact  
946 the emission rate.

947

#### 948 **4.3.5 Intercomparison of methods**

949 In this study, a reliable quantitative intercomparison of the three methods (mobile, tracer and  
950 suction methods) was attempted. A complete comparison of all three methods was possible at  
951 only one out of 20 locations (18 confirmed gas leak locations) because of the long time (>8-10  
952 hrs) needed for full equilibrium of the suction method, whereby emission rates for 7 out of the  
953 8 leaks quantified by the suction method were reported as maxima rather than absolute values  
954 (Table 1). At these 7 locations the emission was thus overestimated.

955 In total, the average CH<sub>4</sub> emissions from natural gas pipeline leaks for the same locations where  
956 we have quantifications from mobile and tracer methods (n = 13) are 2.8 and 1.2 L min<sup>-1</sup>  
957 respectively. The suction method could only be completed at one location. The average  
958 emission rate reported for all the locations from the suction method (high bias due to  
959 incomplete measurement) is 1.2 L min<sup>-1</sup> (n = 8).

960 The higher emission rates derived with the mobile method are in qualitative agreement with  
961 previous studies. Weller et al. (2018) compared quantifications from the mobile measurements  
962 described in von Fischer et al. (2017) with the tracer method and surface enclosure method in  
963 four US cities. They reported that mobile measurement estimates were  $\approx 2.3$  L min<sup>-1</sup> greater  
964 than the tracer method mean estimates of  $\approx 3.2$  L min<sup>-1</sup> (n = 59). This was attributed to the  
965 overestimation of small leaks (< 2.4 L min<sup>-1</sup>) in the mobile measurements method, which we  
966 have also discussed above for our dataset. In addition, performance of only a few transects at  
967 individual locations also lead to systematically high biased emission rate estimates for higher  
968 emission rates (Luetschwager et al., 2021). Indeed, at the locations where we only have one  
969 transects with CH<sub>4</sub> enhancements above the 10% threshold, there is an overestimation from  
970 mobile method compared to the tracer method. For example, at HH001 (n=1), HH015 (n=1)  
971 and HH100 (n=1) the mobile method estimated emissions of a factor 4 higher in comparison  
972 to the tracer method. The analysis of Luetschwager (2019) clearly shows that this high bias is  
973 reduced when numerous transects are performed. Therefore, we carried out multiple transects  
974 to reduce this systematic bias. We note that there are also large differences between the mobile  
975 and tracer methods, e.g. HH002 and HH006. We suspect that the very short gas leak location  
976 distance to the mobile driving transects can explain partially the difference. Moreover,  
977 existence of another leak in the category of A1 at the HH006 location which had to be fixed  
978 prior to the tracer method could explain the difference in emission rate magnitude at this  
979 location. Nevertheless, the limited number of transects and the 10% threshold can contribute  
980 to an overestimation of the average leak rate with the mobile method at an individual location.

981 At the same time, however, the mobile method fails to detect leaks entirely when the leak outlet  
982 is located downwind of the mobile van. The fact that the mobile method misses downwind  
983 emissions constitutes a method specific factor towards biasing city-wide emissions low, which  
984 qualitatively counteracts the high bias above. Generally, the tracer method has higher precision  
985 than the mobile method, but it is more labor intensive. Although the mobile method has lower  
986 precision for emission quantification of individual gas leaks, this method can be implemented  
987 widely in a shorter time frame at a city scale. The mobile method is an empirical statistical  
988 quantification approach based on controlled release experiments, and a large sample size gives  
989 a better estimation in total emission (Weller et al., 2020). Acting on parameters in plume  
990 dispersion, such as distance and wind speed which are not included in the method, mobile  
991 method can overestimate and underestimate individual gas leaks but with a large number of  
992 gas leak quantifications these over- and underestimations may cancel each other out. If (i)  
993 particularly large concurrent subsurface CH<sub>4</sub> and C<sub>2</sub>H<sub>6</sub> accumulations with multiple emission  
994 outlets are observed (this has priority - indication of a large leak) or (ii) a few of the leaks are  
995 significantly larger with small subsurface accumulation than the other leaks, an optimal  
996 approach may be to supplement the mobile method with use of a more precise measurement  
997 method such as the tracer method at those selected locations. The divergence to accurate city-  
998 wide quantification is dependent on urban planning, e.g. width of streets, location of gas  
999 pipelines (under streets or pavements etc.) and emission outlet location (s).

1000

#### 1001 **4.4 Possible sampling bias of suction method toward low gas leak emission locations**

1002 Following our communications with the emission inventory experts (personal communications  
1003 with Christian Böttcher, 2022), we cannot fully reconstruct the methods that are used in the  
1004 existing national inventory report to establish the emission factors due to lack of transparency.  
1005 However, the German environmental agency (UBA) is considering to use the results of the  
1006 recent large scale measurement campaign based on the suction method (MEEM, 2018) in future  
1007 publications of the national emission inventory in Germany (Federal Environment Agency,  
1008 2021). The utilities choose leak locations for application of the suction method where there are  
1009 no safety concerns and/or immediate leak closure is compulsory. This implies that this method  
1010 is not applied at locations of the A1 category, which demand immediate repair (P. 27 in MEEM,  
1011 2018). Due to logistic constraints and the time-consuming nature of the suction measurements,  
1012 they are likely also not (or rarely) applied at locations in the A2 category, which require repair  
1013 within a week. Thus, suction measurements have a location sampling bias towards leaks in the  
1014 B and C category. This is supported by the fact that the leak locations that were contributed by  
1015 the LDC to the intercomparison campaign were locations in the B and C category. This study  
1016 investigated whether this location sampling bias could result in an emission rate bias, which  
1017 could contribute to the fact that the suction method did not report leaks with emission rates as  
1018 high as they have been reported by the mobile method in this study or during previous  
1019 measurements in the same city (Maazallahi et al., 2020).

1020 In this study, emission rates from A1 and A2 category leaks were larger compared to those  
1021 from B and C category leaks (Figure 6). The emission rate differences vary by measurement  
1022 method: a factor 2 for the mobile method (n = 9 for A1&A2, n = 4 for B&C), a factor 11 for  
1023 the tracer method (n = 8 for A1&A2, n = 8 for B&C) and a factor 1.6 for the suction method  
1024 (n=3 for A1&A2, n = 5 B&C). For the mobile method, there is a clear separation between the  
1025 A1&A2 versus the B&C categories. The highest emission estimate for the B&C group  
1026 (HH010) is similar to the lowest emission rate estimate for the A1&A2 group (HH014).  
1027 Furthermore, HH011 in the A1 category was very likely biased low because of the wrongly  
1028 assumed leak location.

1029 For the tracer method, the difference between the two groups is largest, an order of magnitude,  
1030 and we know that emissions are underestimated at least at one location of the A1 category



1031 (HH011). The uncertainty of the tracer method is much smaller than the difference between the  
1032 two groups. The tracer method also illustrates that 4 of the 5 leaks that were contributed by the  
1033 LDC to the intercomparison campaign were extremely small. If these would be representative  
1034 for locations where the suction method is usually applied, it would indeed indicate a severe  
1035 emission rate bias for the suction method, not because the measurements themselves are biased,  
1036 but because locations with low emission rates are targeted with this method. In the  
1037 intercomparison campaign, we attempted to apply the suction method also at locations of the  
1038 A categories, but at 8 out of 9 locations from the A category, the suction measurements could  
1039 not be applied for safety reasons, or suction could not be completed, because of the widespread  
1040 subsurface accumulation (Table 2). At the other A location (HH014), the suction method could  
1041 not be applied as the ground had been already opened for the repair.  
1042

## 1043 **5 Conclusion**

1044  
1045 In summer 2020, we compared three gas leak rate quantification methods, namely the mobile,  
1046 tracer, and suction methods, in Hamburg, Germany. While the mobile and tracer methods have  
1047 been compared previously, this is the first peer-reviewed study that includes the suction  
1048 method, although suction measurements could not be completed in one day at most locations.  
1049 The mobile method can cover large areas in a short time, but some of the smaller leaks ( $< 0.5$   
1050  $\text{L min}^{-1}$ ) are not identified as a gas leak location due to the 10% enhancement threshold in the  
1051 standard mobile quantification algorithm. While the mobile method quantification algorithm is  
1052 designed to accurately report city-level total gas distribution leak rates (i.e., considering a large  
1053 sample size), it has large (known) uncertainties for individual leaks. The tracer method has a  
1054 smaller uncertainty, but it is labor intensive in comparison to the mobile method. On average,  
1055  $\text{CH}_4$  emissions from natural gas pipeline leaks were higher from mobile quantifications in  
1056 comparison to tracer quantifications. For many locations, we encountered several outlets and  
1057 with widespread underground gas accumulations. At one location, after deployment of the  
1058 mobile and the tracer quantification and during the repair actions, it was found out that the  
1059 actual leak in the gas pipeline was located  $\approx 60$  m away from the identified emission outlet  
1060 indicating significant underground gas migration. It is possible that this leak had several  
1061 emission outlets that were not identified and the emission quantified from the single outlet is  
1062 thus not representative for the whole emission from this leak.

1063 The suction method has a low reported uncertainty, but it is even more labor and time intensive  
1064 than the tracer method. Due to the time and effort needed to plan and execute the measurements,  
1065 the suction method is likely never applied in routine operation at A1 or A2 safety category  
1066 leaks that mandate immediate or near-time repair. In our study, it was also not feasible to apply  
1067 the suction method at locations with large subsurface  $\text{CH}_4$  accumulations. Our results thus  
1068 indicate a systematic difference between A1 and A2 (high emissions) versus B and C (low  
1069 emissions) category locations, and generally larger emission rates are inferred with the mobile  
1070 and tracer methods for sites with widespread subsurface accumulation.

1071 This study did not allow a direct, quantitative comparison of emission rates estimated with all  
1072 three different methods because of the inability to quantify the same leak locations with all  
1073 methods. However, this inability illuminates the importance of site selection for deriving  
1074 representative emission factors based on empirical measurements. Specifically, the results  
1075 suggest that a significant emission rate bias could exist for measurements that are carried out  
1076 with the suction method. Our results therefore stipulate that representative site selection  
1077 includes sampling at all leak safety categories (MEEM, 2018). Otherwise, this could lead to a  
1078 sampling and emission rate bias in the national inventory of gas leak  $\text{CH}_4$  emission in Germany.  
1079

1080 **Authors contributions:** TR, HM and SS conceived and designed the study. TR coordinated  
1081 the campaign in collaboration with DBI, Technical University of Denmark (DTU),  
1082 Environmental Defense Fund (EDF), E.On and Gasnetz Hamburg (GNH) teams. HM carried  
1083 out the mobile measurements, emission outlet attribution, performed the analyses of mobile  
1084 data and collectively with TR analyzed the intercomparison results. AD, CS and AMF  
1085 performed the tracer method and reported the emission rates from the tracer dataset.  
1086 HDvdG and TR made instruments and equipment available for the mobile method and CS  
1087 provided those for the tracer method. HM wrote the paper, and all co-authors supported the  
1088 interpretation of the results and contributed to improving the paper.

1090 **Competing interests:** The authors declare that they have no conflict of interest.

### 1092 **Acknowledgement**

1093 This study was carried out with the financial support from the Environmental Defense Fund.  
1094 Extra financial supports were provided by the H2020 Marie Skłodowska-Curie actions through  
1095 Methane goes Mobile – Measurements and Modelling project (MEMO<sup>2</sup>; [https://h2020-](https://h2020-memo2.eu/)  
1096 [memo2.eu/](https://h2020-memo2.eu/), last access: 20 April 2022), grant number 722479. In this study, Robertson  
1097 Foundation supported contribution of Stefan Schwietzke. We appreciate efforts from  
1098 Luise Westphal, Michael Dammann, Ralf Luy, Christian Feickert, Volker Krell, Turhan Ulas,  
1099 Dieter Bruhns and Sönke Graumann, from GasNetz Hamburg GmbH who facilitated this study  
1100 by hosting the teams, arranging and applying the carpet method leak detection and confirmation  
1101 procedures, making information on gas leaks and pipelines available for the data analysis and  
1102 applying leak repair protocols. We extend our appreciation to Andre Lennartz, Stefan Gollanek  
1103 and Dieter Wolf from E.On-for their contribution in the planning of the campaign, deploying  
1104 the suction method at the locations, and exchanging their knowledge and experiences from  
1105 their previous campaigns. We thank the team from DBI Gas and Environmental  
1106 Technologies GmbH Leipzig (DBI GUT Leipzig) including Charlotte Große, who contributed  
1107 to providing information for structuring the campaign planning.

## 1109 **Reference:**

- 1110 Alvarez, R. A., Pacala, S. W., Winebrake, J. J., Chameides, W. L., Hamburg, S. P.: Greater  
1111 focus needed on methane leakage from natural gas infrastructure, PNAS, 109 (17)  
1112 6435-6440, <https://doi.org/10.1073/pnas.1202407109>, 2012.
- 1113 Ars, S., Vogel, F., Arrowsmith, C., Heerah, S., Knuckey, E., Lavoie, J., Lee, C., Mostafavi Pak,  
1114 N., Phillips, J. L., and Wunch, D., Investigation of the Spatial Distribution of Methane  
1115 Sources in the Greater Toronto Area Using Mobile Gas Monitoring Systems, Environ.  
1116 Sci. Technol., 54, 24, 15671–15679, <https://doi.org/10.1021/acs.est.0c05386>, 2020.
- 1117 Allwine G., Lamb B., Westberg H., Application of Atmospheric Tracer Techniques for  
1118 Determining Biogenic Hydrocarbon Fluxes from an Oak Forest. In: Hutchison B.A.,  
1119 Hicks B.B. (eds) The Forest-Atmosphere Interaction. Springer, Dordrecht.  
1120 [https://doi.org/10.1007/978-94-009-5305-5\\_23](https://doi.org/10.1007/978-94-009-5305-5_23), 1985.
- 1121 Arnaldos, J., Casal, J., Montiel, H., Sánchez-Carricondo, M., Vílchez, J.A., Design of a  
1122 computer tool for the evaluation of the consequences of accidental natural gas releases  
1123 in distribution pipes, Journal of Loss Prevention in the Process Industries,  
1124 [https://doi.org/10.1016/S0950-4230\(97\)00041-7](https://doi.org/10.1016/S0950-4230(97)00041-7), 1998.
- 1125 Bousquet, P., Ciais, P., Miller, J. B., Dlugokencky, E. J., Hauglustaine, D. A., Prigent, C., Van  
1126 der Werf, G. R., Peylin, P., Brunke, E. G., Carouge, C., Langenfelds, R. L., Lathière,  
1127 J., Papa, F., Ramonet, M., Schmidt, M., Steele, L. P., Tyler, S. C., White, J.,

1128 Contribution of anthropogenic and natural sources to atmospheric methane variability.  
1129 Nature.; 443(7110):439-43. <https://doi.org/10.1038/nature05132>, 2006.

1130 Brandt, A. R., Heath, G. A., and Cooley, D., Methane Leaks from Natural Gas Systems Follow  
1131 Extreme Distributions, Environmental Science & Technology, 50 (22), 12512-12520,  
1132 <https://doi.org/10.1021/acs.est.6b04303>, 2016

1133 Cho, Y., Ulrich, B. A., Zimmerle, D. J., Smits, K. M., Estimating natural gas emissions from  
1134 underground pipelines using surface concentration measurements, Environmental  
1135 Pollution, <https://doi.org/10.1016/j.envpol.2020.115514>, 2020.

1136 Defratyka, S. M., Paris, J. D., Yver-Kwok, C., Fernandez, J. M., Korben, P., and Bousquet, P.,  
1137 Environmental Science & Technology Article ASAP,  
1138 <https://doi.org/10.1021/acs.est.1c00859>, 2021.

1139 Delre, A., Greenhouse gas emissions from wastewater treatment plants: measurements and  
1140 carbon footprint assessment, Ph.D. Thesis, Department of Environmental Engineering,  
1141 Technical University of Denmark (DTU), Copenhagen, Available at:  
1142 [https://orbit.dtu.dk/en/publications/greenhouse-gas-emissions-from-wastewater-](https://orbit.dtu.dk/en/publications/greenhouse-gas-emissions-from-wastewater-treatment-plants-measure)  
1143 [treatment-plants-measure](https://orbit.dtu.dk/en/publications/greenhouse-gas-emissions-from-wastewater-treatment-plants-measure) (Last Accessed: 15 June 2021), 2018.

1144 DVGW: High-performing infrastructure, (2022). [online] Available from  
1145 <https://www.dvgw.de/english-pages/topics/safety-and-security/technical-safety-gas>,  
1146 (Last Accessed: 25 January 2022)

1147 DVGW: Technische Regel-Arbeitsblatt; DVGW G465-1 (A) (2019). [online] Available from:  
1148 [https://shop.wvgw.de/var/assets/leseprobe//510544\\_lp\\_G\\_465-1\\_2019\\_05.pdf](https://shop.wvgw.de/var/assets/leseprobe//510544_lp_G_465-1_2019_05.pdf). (Last  
1149 Accessed: 15 December 2021)

1150 Ebrahimi-Moghadam, A., Farzaneh-Gord, M., Arabkoohsar, A., Jabari Moghadam, A., CFD  
1151 analysis of natural gas emission from damaged pipelines: Correlation development for  
1152 leakage estimation, Cleaner Production, <https://doi.org/10.1016/j.jclepro.2018.07.127>,  
1153 2018.

1154 EC: EU strategy to reduce methane emissions available at: [https://eur-lex.europa.eu/legal-](https://eur-lex.europa.eu/legal-content/EN/TXT/?uri=CELEX%3A52020DC0663&qid=1644853088591)  
1155 [content/EN/TXT/?uri=CELEX%3A52020DC0663&qid=1644853088591](https://eur-lex.europa.eu/legal-content/EN/TXT/?uri=CELEX%3A52020DC0663&qid=1644853088591), (last  
1156 access: 28 March 2022), 2020

1157 EIA, Carbon Dioxide Emissions Coefficients, available at:  
1158 [https://www.eia.gov/environment/emissions/co2\\_vol\\_mass.php](https://www.eia.gov/environment/emissions/co2_vol_mass.php), (last access:  
1159 28 March 2022), 2021.

1160 EPA, Methane emissions from the natural gas industry: underground pipelines,  
1161 [https://www.epa.gov/sites/production/files/2016-08/documents/9\\_underground.pdf](https://www.epa.gov/sites/production/files/2016-08/documents/9_underground.pdf),  
1162 1996.

1163 Federal Environment Agency: National Inventory Report for the German Greenhouse Gas  
1164 Inventory 1990–2019, available at: <https://unfccc.int/documents/194930>, (last access:  
1165 15 December 2022), 2021.

1166 Fernandez, J. M., Maazallahi, H., France, J. L., Menoud, M., Corbu, M., Ardelean, M., Calcan,  
1167 A., Townsend-Small, A., van der Veen, C., Fisher, R. E., Lowry, D., Nisbet, E.G.,  
1168 Röckmann, T.: Street-level methane emissions of Bucharest, Romania and the  
1169 dominance of urban wastewater., Atmospheric Environment: X, 13, 2590-1621,  
1170 100153, <https://doi.org/10.1016/j.aeaoa.2022.100153>, 2022.

1171 Fredenslund, A.M., Scheutz, C., Kjeldsen, P.: Tracer method to measure landfill gas emissions  
1172 from leachate collection systems, Waste Management, 30, 2146-2152,  
1173 <https://doi.org/10.1016/j.wasman.2010.03.013>, 2010

1174 Fredenslund, A. M., Rees-White, T. C., Beaven, R. P., Delre, A., Finlayson, A., Helmore, J.,  
1175 Allen, G., Scheutz, C.: Validation and error assessment of the mobile tracer gas  
1176 dispersion method for measurement of fugitive emissions from area sources, Waste  
1177 Management, 83, 68-78, <https://doi.org/10.1016/j.wasman.2018.10.036>, 2019.

1178 Federal Environment Agency: National Inventory Report for the German Greenhouse Gas  
 1179 Inventory 1990 – 2018, available at: <https://unfccc.int/documents/226313> (last access:  
 1180 30 March 2022), 2020.

1181 Hendrick, M. F., Ackle, R., Sanaie-Movahed, B., Tang, X., Phillips, N. G., Fugitive methane  
 1182 emissions from leak-prone natural gas distribution infrastructure in urban  
 1183 environments, *Environmental Pollution*, <https://doi.org/10.1016/j.envpol.2016.01.094>,  
 1184 2016.

1185 Hou, Q., Yang, D., Li, X., Xiao, G. and Ho, S. C. M., Modified Leakage Rate Calculation  
 1186 Models of Natural Gas Pipelines, *Mathematical Problems in Engineering*,  
 1187 <https://doi.org/10.1155/2020/6673107>, 2020.

1188 Jackson, R. B., Saunio, M., Bousquet, P., Canadell, J. G., Poulter, B., Stavert, A. R.,  
 1189 Bergamaschi, P., Niwa, Y., Segers, A. and Tsuruta, A., Increasing anthropogenic  
 1190 methane emissions arise equally from agricultural and fossil fuel sources,  
 1191 *Environmental Research Letters*, 15, 071002, <https://doi.org/10.1088/1748-9326/ab9ed2>, 2020.

1193 Jackson, R. B., Down, A., Phillips, N. G., Ackley, R. C., Cook, C. W., Plata, D. L., and Zhao,  
 1194 K., Natural Gas Pipeline Leaks Across Washington, DC, *Environ. Sci. Technol.*, 48, 3,  
 1195 2051–2058, <https://doi.org/10.1021/es404474x>, 2014.

1196 Kirchgessner, D. A., Lott R. A., Cowgill, R.M., Harrison, M. R., Shires, T. M., Estimate of  
 1197 methane emissions from the U.S. natural gas industry, *Chemosphere*,  
 1198 [https://doi.org/10.1016/S0045-6535\(97\)00236-1](https://doi.org/10.1016/S0045-6535(97)00236-1), 1997.

1199 Keyes, T., Ridge G., Klein, M., Phillips, N., Ackley, R., Yang Y., An enhanced procedure for  
 1200 urban mobile methane leak detection. *Heliyon*. 9; 6 (10):e04876.  
 1201 <https://doi.org/10.1016/j.heliyon.2020.e04876>, 2020.

1202 Lamb, B. K., McManus, J. B., Shorter, J. H., Kolb, C. E., Mosher, B., Harriss, R. C., Allwine,  
 1203 E., Blaha, D., Howard, T., Guenther, A., Lott, R. A., Siverson, R., Westburg, H., and  
 1204 Zimmerman, P., Development of atmospheric tracer methods to measure methane  
 1205 emissions from natural gas facilities and urban areas, *Environmental Science &*  
 1206 *Technology* 29 (6), 1468-1479 <https://doi.org/10.1021/es00006a007>, 1995.

1207 Lamb, B. K., Edburg, S. L., Ferrara, T. W., Howard, T., Harrison, M. R., Kolb, C. E.,  
 1208 Townsend-Small, A., Dyck, W., Possolo, A., and Whetstone, J. R., *Environmental*  
 1209 *Science & Technology* 49 (8), 5161-5169 <https://doi.org/10.1021/es505116p>, 2015.

1210 Luetschwager, E., von Fischer, J. C., Weller, Z. D., Characterizing detection probabilities of  
 1211 advanced mobile leak surveys: Implications for sampling effort and leak size estimation  
 1212 in natural gas distribution systems. *Elementa: Science of the Anthropocene*; 9 (1):  
 1213 00143. <https://doi.org/10.1525/elementa.2020.00143>, 2021.

1214 Liu, C., Liao, Y., Liang, J., Cui, Z., Li, Y., Quantifying methane release and dispersion  
 1215 estimations for buried natural gas pipeline leakages, *Process Safety and Environmental*  
 1216 *Protection*, <https://doi.org/10.1016/j.psep.2020.11.031>, 2021.

1217 Maazallahi, H., Fernandez, J. M., Menoud, M., Zavala-Araiza, D., Weller, Z. D., Schwietzke,  
 1218 S., von Fischer, J. C., Denier van der Gon, H., and Röckmann, T.: Methane mapping,  
 1219 emission quantification, and attribution in two European cities: Utrecht (NL) and  
 1220 Hamburg (DE), *Atmos. Chem. Phys.*, 20, 14717–14740, <https://doi.org/10.5194/acp-20-14717-2020>, 2020.

1222 Mahgerefteh, H., Oke, A., Atti, O., Modelling outflow following rupture in pipeline networks,  
 1223 *Chemical Engineering Science*, <https://doi.org/10.1016/j.ces.2005.10.013>, 2006.

1224 MEEM, Methane emission estimation method for the gas distribution grid, [Online], Available  
 1225 from: [https://www.dbi-  
 1226 gut.de/emissions.html?file=files/PDFs/Emissionen/Final%20Report\\_MEEM%20DSO  
 1227 \\_end\\_signed.pdf&cid=5804](https://www.dbi-gut.de/emissions.html?file=files/PDFs/Emissionen/Final%20Report_MEEM%20DSO_end_signed.pdf&cid=5804). (Last Accessed: 12 December 2022), 2018.

1228 Moloudi, R., Abolfazli Esfahani, J., Modeling of gas release following pipeline rupture:  
1229 Proposing non-dimensional correlation, *Journal of Loss Prevention in the Process*  
1230 *Industries*, <https://doi.org/10.1016/j.jlp.2014.09.003>, 2014.

1231 Mønster, J. G., Samuelsson, J., Kjeldsen, P., Rella, C. W., Scheutz, C., Quantifying methane  
1232 emission from fugitive sources by combining tracer release and downwind  
1233 measurements – A sensitivity analysis based on multiple field surveys, *Waste*  
1234 *Management*, 34, 1416-1428, <https://doi.org/10.1016/j.wasman.2014.03.025>, 2014.

1235 Myhre, G., Shindell, D., Bréon, F. M., Collins, W., Fuglestvedt, J., Huang, J., Koch, D.,  
1236 Lamarque, J. F., Lee, D., Mendoza, B., Nakajima, T., Robock, A., Stephens, G.,  
1237 Takemura, T., and Zhan, H.: Anthropogenic and Natural Radiative Forcing, in:  
1238 *Climate Change 2013: The Physical Science Basis, Contribution of Working Group I*  
1239 *to the Fifth Assessment Report of the Intergovernmental Panel on Climate Change*,  
1240 Cambridge, UK and New York, NY, USA, available at:  
1241 [https://www.ipcc.ch/site/assets/uploads/2018/02/WG1AR5\\_Chapter08\\_FINAL.pdf](https://www.ipcc.ch/site/assets/uploads/2018/02/WG1AR5_Chapter08_FINAL.pdf),  
1242 2013.

1243 Nisbet, E. G., Manning, M. R., Dlugokencky, E. J., Fisher, R. E., Lowry, D., Michel, S. E.,  
1244 Myhre, C. L., Platt, S. M., Allen, G., Bousquet, P., Brownlow, R., Cain, M., France, J.  
1245 L., Hermansen, O., Hossaini, R., Jones, A. E., Levin, I., Manning, A. C., Myhre, G.,  
1246 Pyle, J. A., Vaughn, B. H., Warwick, N. J., White, J. W. C., Very strong atmospheric  
1247 methane growth in the 4 Years 2014–2017: implications for the Paris agreement, *Global*  
1248 *Biogeochemical Cycles*, 33, 318 – 342, <https://doi.org/10.1029/2018GB006009>, 2019.

1249 Okamoto, H., Gomi, Y., Empirical research on diffusion behavior of leaked gas in the ground,  
1250 *Journal of Loss Prevention in the Process Industries*,  
1251 <https://doi.org/10.1016/j.jlp.2011.01.007>, 2011.

1252 Phillips, N. G., Ackley, R., Crosson, E. R., Down, A., Hutyra, L. R., Brondfield, M., Karr, J.  
1253 D., Zhao, K., Jackson, R. B., Mapping urban pipeline leaks: Methane leaks across  
1254 Boston, *Environmental Pollution*, 173, 1-4,  
1255 <https://doi.org/10.1016/j.envpol.2012.11.003>, 2013.

1256 Scheutz, C., Samuelsson, J., Fredenslund, A.M., Kjeldsen, P., Quantification of multiple  
1257 methane emission sources at landfills using a double tracer technique, *Waste*  
1258 *Management*, 31, 1009-1017, <https://doi.org/10.1016/j.wasman.2011.01.015>, 2011.

1259 Ulrich, B. A., Mitton, M., Lachenmeyer, E., Hecobian, A., Zimmerle, D., and Smits, K. M.,  
1260 Natural Gas Emissions from Underground Pipelines and Implications for Leak  
1261 Detection, *Environmental Science & Technology Letters*, 6 (7), 401-406,  
1262 <https://doi.org/10.1021/acs.estlett.9b00291>, 2019.

1263 Von Fischer, J. C., Cooley, D., Chamberlain, S., Gaylord, A., Griebenow, C. J., Hamburg, S.  
1264 P., Salo, J., Schumacher, R., Theobald, D., and Ham, J.: Rapid, Vehicle-Based  
1265 Identification of Location and Magnitude of Urban Natural Gas Pipeline Leaks,  
1266 *Environ. Sci. Technol.*, 51, 4091–4099, <https://doi.org/10.1021/acs.est.6b06095>, 2017.

1267 Weller, Z. D., Roscioli, J. R., Daube, W. C., Lamb, B. K., Ferrara, T. W., Brewer, P. E., and  
1268 von Fischer, J. C.: Vehicle-Based Methane Surveys for Finding Natural Gas Leaks and  
1269 Estimating Their Size: Validation and Uncertainty, *Environ. Sci. Technol.*, 52, 11922–  
1270 11930, <https://doi.org/10.1021/acs.est.8b03135>, 2018.

1271 Weller, Z. D., Yang, D. K., and von Fischer, J. C.: An open source algorithm to detect natural  
1272 gas leaks from mobile methane survey data, edited by: Mauder, M., *PLoS One*, 14,  
1273 e0212287, <https://doi.org/10.1371/journal.pone.0212287>, 2019.

1274 Weller, Z. D., Hamburg, S. P., and von Fischer, J. C., A National Estimate of Methane Leakage  
1275 from Pipeline Mains in Natural Gas Local Distribution Systems, *Environmental*  
1276 *Science & Technology*, 54 (14), 8958-8967, <https://doi.org/10.1021/acs.est.0c00437>,  
1277 2020

1278 Wiesner, S., Gröngröft, A., Ament, F. et al. Spatial and temporal variability of urban soil water  
1279 dynamics observed by a soil monitoring network. *J Soils Sediments* 16, 2523–2537.  
1280 <https://doi.org/10.1007/s11368-016-1385-6>, 2016  
1281 Worden, J. R., Anthony Bloom, A., Pandey, S., Jiang, Z., Worden, H. M., Walker, T. W.,  
1282 Houweling, S., Röckmann, T., , Reduced biomass burning emissions reconcile  
1283 conflicting estimates of the post-2006 atmospheric methane budget, *Nature*  
1284 *Communications* 8, 2227 <https://doi.org/10.1038/s41467-017-02246-0>, 2017  
1285 Yan, Y., Dong, X., Li, J., Experimental study of methane diffusion in soil for an underground  
1286 gas pipe leak, *Journal of Natural Gas Science and Engineering*,  
1287 <https://doi.org/10.1016/j.jngse.2015.08.039>, 2015.  
1288 Yuhua, D., Huilin, G., Jing'en, Z., Yaorong, F., Evaluation of gas release rate through holes in  
1289 pipelines, *Journal of Loss Prevention in the Process Industries*,  
1290 [https://doi.org/10.1016/S0950-4230\(02\)00041-4](https://doi.org/10.1016/S0950-4230(02)00041-4), 2002.  
1291